

TALLINN UNIVERSITY OF TECHNOLOGY
DOCTORAL THESIS
19/2019

**Flow Sensing with Pressure Sensor-Based
Artificial Lateral Lines: from the
Laboratory to the Field**

JUAN FRANCISCO FUENTES-PÉREZ



TALLINN UNIVERSITY OF TECHNOLOGY

School of Information Technologies

Department of Computer Systems

This dissertation was accepted for the defence of the degree 01/04/2019

Supervisor:

Prof. Maarja Kruusmaa
School of Information Technologies
Tallinn University of Technology
Tallinn, Estonia

Co-supervisor:

Dr.-Eng. Jeffrey A. Tuhtan
School of Information Technologies
Tallinn University of Technology
Tallinn, Estonia

Opponents:

Prof. Asgeir Johan Sørensen
Faculty of Engineering
Department of Marine Technology
Norwegian University of Science and Technology
Trondheim, Norway

Prof. Dr.-Ing. habil. Boris Lehmann
Department of Hydraulic Engineering and Water
Management
Technical University Darmstadt
Darmstadt, Germany

Defence of the thesis: 14/05/2019, Tallinn

Declaration:

Hereby I declare that this doctoral thesis, my original investigation and achievement, submitted for the doctoral degree at Tallinn University of Technology has not been submitted for doctoral or equivalent academic degree.

Juan Francisco Fuentes-Pérez

signature



European Union
European Regional
Development Fund



Investing
in your future

Copyright: Juan Francisco Fuentes-Pérez, 2019

ISSN 2585-6898 (publication)

ISBN 978-9949-83-420-4 (publication)

ISSN 2585-6901 (PDF)

ISBN 978-9949-83-421-1 (PDF)

TALLINNA TEHNIKAÜLIKOO
DOKTORITÖÖ
19/2019

**Veevoolu tajumine rõhusensoritel
baseeruvate küljejooneanduritega: laborist
välikatseteni**

JUAN FRANCISCO FUENTES-PÉREZ

Contents

Contents	5
List of Publications	7
Other related journal publications.....	8
Author’s Contribution to the Publications	10
Abbreviations	11
Symbols	12
Introduction	13
Motivation.....	14
Problem statement and methodological approach	15
Specific contributions of the thesis.....	21
Outline of the thesis.....	22
1. General background.....	23
1.1. Artificial lateral lines	23
1.1.1. Types of ALLs	24
1.1.2. Absolute and gauge pressure sensor-based ALLs.....	26
1.1.3. Differential pressure sensor-based ALLs	29
1.2. Applications of ALLs	32
1.2.1. Hydrodynamic variable estimation using pressure sensing	34
1.3. Summary and conclusions	35
2. Flow sensing with absolute pressure sensor-based ALLs	36
2.1. The studied prototype	36
2.2. Studied scenarios.....	37
2.3. Hydrodynamic variable estimation approaches	39
2.3.1. Classical approach and its limitations.....	39
2.3.2. Mixed approach.....	40
2.3.3. Statistical approaches.....	43
2.3.4. Neural network approach.....	43
2.4. Method Comparison	44
2.5. Map based localization using hydrodynamic variables.....	47
2.6. Summary and conclusions	50
3. Development of differential pressure sensor-based ALLs	51
3.1. Prototype development.....	51
3.1.1. Shape	51
3.1.2. Sensors and electronics	52
3.1.3. First physical prototype	53
3.2. Performance evaluation.....	54
3.3. Developed ALLs prototypes	56
3.3.1. D-Box	56
3.3.2. iRon.....	56
3.3.3. DPSS.....	57
3.4. Summary and conclusions	58
4. Applications of differential pressure sensor-based ALLs	59
4.1. Underwater velocity estimation	59
4.2. Fish preferences.....	62
4.3. Summary and conclusions	67
Conclusions and future outlook.....	68
Future outlook	69

References	71
Acknowledgements.....	78
Abstract.....	79
Lühikokkuvõte.....	81
Appendix 1	83
Appendix 2	91
Appendix 3	107
Appendix 4	117
Appendix 5	127
Appendix 6	135
Appendix 7	147
Appendix 8	157
Curriculum vitae.....	168
Elulookirjeldus.....	169

List of Publications

The work of this thesis is based on the following publications:

- I **Fuentes-Pérez, J. F.**, Tuhtan, J. A., Carbonell-Baeza, R., Musall, M., Toming, G., Muhammad, N., & Kruusmaa, M. (2015). Current velocity estimation using a lateral line probe. *Ecological Engineering*, 85, 296–300. DOI: 10.1016/j.ecoleng.2015.10.008.
- II Strokina, N., Kämäräinen, J. K., Tuhtan, J. A., **Fuentes-Pérez, J. F.**, & Kruusmaa, M. (2016). Joint estimation of bulk flow velocity and angle using a lateral line probe. *IEEE Transactions on Instrumentation and Measurement*, 65(3), 601–613. DOI: 10.1109/TIM.2015.2499019.
- III Tuhtan, J. A., **Fuentes-Pérez, J. F.**, Strokina, N., Toming, G., Musall, M., Noack, M., Kämäräinen, J. K., & Kruusmaa, M. (2016). Design and application of a fish-shaped lateral line probe for flow measurement. *Review of Scientific Instrumentation*, 87, 045110. DOI: 10.1063/1.4946765.
- IV Tuhtan, J. A., **Fuentes-Pérez, J. F.**, Toming, G., & Kruusmaa, M. (2017). Flow velocity estimation using a fish-shaped lateral line probe with product-moment correlation features and a neural network. *Flow Measurement and Instrumentation*, 54, 1–8. DOI: 10.1016/j.flowmeasinst.2016.10.017
- V **Fuentes-Pérez, J. F.**, Kalev, K., Tuhtan, J. A., & Kruusmaa, M. (2016). Underwater vehicle speedometry using differential pressure sensors: Preliminary results. *IEEE OES Autonomous Underwater Vehicles*. DOI: 10.1109/AUV.2016.7778664.
- VI Chen, K., Tuhtan, J. A., **Fuentes-Pérez, J. F.**, Toming, G., Musall, M., Strokina, N., Kämäräinen, J. K., & Kruusmaa, M. (2017). Estimation of flow turbulence metrics with a lateral line probe and regression. *IEEE Transactions on Instrumentation and Measurement*, 66(4), 651–660 DOI: 10.1109/TIM.2017.2658278.
- VII **Fuentes-Pérez, J. F.**, Muhammad, N., Tuhtan, J. A., Carbonell-Baeza, R., Musall, M., Toming, G., & Kruusmaa, M. (2017). Map-based localization in structured underwater environment using simulated hydrodynamic maps. *IEEE ROBIO 2017*. DOI: 10.1109/ROBIO.2017.8324406.
- VIII **Fuentes-Pérez, J. F.**, Meurer, C., Tuhtan, J. A., & Kruusmaa, M. (2018). Differential pressure sensors for underwater speedometry in variable velocity and acceleration conditions. *IEEE OES Journal of Oceanic Engineering*. DOI: 10.1109/JOE.2017.2767786.

Other related journal publications

List of journal publications that this thesis is not directly based on but where the author of the thesis has contributed during the dissertation period as an author. Conference papers are not included. A complete list of publications can be consulted in the Estonian Research Information System account of the author (www.etis.ee) or the CV available in the personal web page of the author (www.fuentesperez.com).

1. Musall, M., Oberle, P., Baeza, R. C., **Fuentes-Pérez, J. F.**, Tuhtan, J. A., & Nestmann, F. (2015). Comments on the Detailed Analysis of Vertical Slot Fishway Hydraulics. *WASSERWIRTSCHAFT*, 105(7-8), 67-72. DOI: 10.1007/s35147-015-0551-x.
2. **Fuentes-Pérez, J. F.**, Navarro Hevia, J., Ruiz Legazpi, J., & García-Vega, A. (2015). Inventario y caracterización morfológica de lagos y lagunas de alta montaña en las provincias de Palencia y León (España). *Pirineos*, 170. DOI: 10.3989/Pirineos.2015.170006.
3. **Fuentes-Pérez, J. F.**, Sanz-Ronda, F. J., Martínez de Azagra, A., & García-Vega, A. (2016). Non-uniform hydraulic behavior of pool-weir fishways: a tool to optimize its design and performance. *Ecological Engineering*, 86, 5–12. DOI: 10.1016/j.ecoleng.2015.10.021.
4. Sanz-Ronda, F. J., Bravo-Córdoba, F. J., **Fuentes-Pérez, J. F.**, Castro-Santos, T. (2016). Ascent ability of brown trout, *Salmo trutta*, and two Iberian cyprinids - Iberian barbel, *Luciobarbus bocagei*, and northern straight-mouth nase, *Pseudochondrostoma duriense* - in a vertical slot fishway. *Knowledge and Management of Aquatic Ecosystems*, 10. DOI: 10.1051/kmae/2015043.
5. García-Vega, A., Sanz-Ronda, F. J., & **Fuentes-Pérez, J. F.** (2017) Seasonal and daily upstream movements of brown trout *Salmo trutta* in an Iberian regulated river. *Knowledge and Management of Aquatic Ecosystems*, 418, 6. DOI: 10.1051/kmae/2016041.
6. Schletterer, M., Kuzovlev, V.V., Zhenikov, Y.N., Tuhtan, J. A., **Fuentes-Perez J. F.** (2017). Classification of benthic biocenosis of the lowland river Tudovka (Tver Region, Russia) using community features. *Geography, Environment, Sustainability*. DOI: 10.24057/2071-9388-2017-10-2-40-56.
7. **Fuentes-Pérez, J. F.**, García-Vega, A., Sanz-Ronda, F. J., & Martínez de Azagra, A. (2017). Villemonte's approach: validation of a general method for modeling uniform and non-uniform performance in stepped fishways. *Knowledge and Management of Aquatic Ecosystems*. 418, 23. DOI: 10.1051/kmae/2017013.
8. Thumser, P., Haas, C., Tuhtan, J. A., **Fuentes-Pérez, J. F.** & Toming, G. (2017). RAPTOR-UAV: Real-Time Particle Tracking in Rivers using an Unmanned Aerial Vehicle. *Earth Surface Processes and Landforms*. DOI: 10.1002/esp.4199.
9. **Fuentes-Pérez, J. F.**, Silva, A. T., Tuhtan, J. A., García-Vega, A., Carbonell-Baeza, R., Musall, M., & Kruusmaa, M. (2018). 3D modeling of non-uniform and turbulent flow in vertical slot fishways. *Environmental Modelling & Software*. 99C, pp. 156–169. DOI: 10.1016/j.envsoft.2017.09.011.

10. Tuhtan, J. A., **Fuentes-Pérez, J. F.**, Toming, G., Schneider, M., & Schletterer, M. (2018). A fish is not a point: analyses of innatural hydrodynamic signatures in fish migration facilities, using a fish-shaped lateral line probe. *WASSERWIRTSCHAFT*, Ausgabe 2–3. DOI: 10.1007/s35147-018-0015-1.
11. Ruiz-Legazpi, J., Sanz-Ronda, F.J., Bravo-Córdoba, F.J., **Fuentes-Pérez, J. F.**, & Castro-Santos, T. (2018). Influencia de factores ambientales y biométricos en la capacidad de nado del barbo ibérico (*Luciobarbus bocagei* steindachner, 1864), un ciprínido potamódromo endémico de la Península Ibérica. *Limnetica*. DOI: 10.23818/limn.37.20.
12. Tuhtan, J. A., **Fuentes-Pérez, J. F.**, Toming, G., Schneider, M., Schwarzenberger, R., Schletterer, M., & Kruusmaa, M., (2018). Man-made flows from a fish's perspective: autonomous classification of turbulent fishway flows with field data collected using an artificial lateral line. *Bioinspiration & Biomimetics*. DOI: 10.1088/1748-3190/aabc79
13. Muhammad, N., **Fuentes-Pérez, J. F.**, Tuhtan, J. A., Toming, G., Musall, M., & Kruusmaa, M. (2018). Map-based localization and loop-closure detection from a moving underwater platform using flow features. *Autonomous Robots*. DOI: 10.1007/s10514-018-9797-3.
14. **Fuentes-Pérez, J. F.**, Eckert, M., Tuhtan, J. A., Ferreira, M.T., Kruusmaa, M., & Branco, P., (2018). Spatial preferences of Iberian barbel in a vertical slot fishway under variable hydrodynamic scenarios. *Ecological Engineering*. DOI: 10.1016/j.ecoleng.2018.10.014
15. **Fuentes-Pérez, J. F.**, Tuhtan, J. A., Eckert, M., Romão, F., Ferreira, M. T., Kruusmaa, M., & Branco, P., (2019). Hydraulics of vertical slot fishways: Non-uniform profiles. *Journal of Hydraulic Engineering*. DOI: 10.1061/(ASCE)HY.1943-7900.0001565.
16. Costa, M., **Fuentes-Pérez, J. F.**, Boavida, I., Tuhtan, J. A., & Pinheiro, A.N. (2019). Fish under pressure: examining behavioural responses of Iberian barbel under simulated hydropeaking with instream structures. *Plos One*. DOI: 1–10.10.1371/journal.pone.0211115.
17. Meurer, C., **Fuentes-Pérez, J. F.**, Palomeras, N., Carreras, M., & Kruusmaa, M. (2019). Differential Pressure Sensor Speedometer for AUV velocity estimation. *IEEE Journal of Oceanic Engineering* (in Press).
18. Boavida, I., Díaz-Redondo, M., **Fuentes-Pérez, J. F.**, Hayes, D. S., Jesus, J., Moreira, M., Belmar, O., Vila-Martínez, N., Palau-Nadal, A., & Costa, M. J. (2019). Ecohydraulics in the global context of river flow alterations and impacts for freshwater fish. *Limnetica* (in Press).

Author's Contribution to the Publications

The contributions of the author to the papers in this thesis are as follows:

- I Participated in the definition of the research problem, planned and partially conducted the experiments, analyzed the data, developed the algorithms for the current estimation, discussed the results, and co-wrote the article.
- II Designed and conducted the experiments and participated in the writing process.
- III Planned and partially conducted the experiments, designed part of the algorithms, and participated in the analysis of the results, the discussion of the data, and the writing process.
- IV Participated in the experimental design, conducted part of the experiments, developed the algorithm for Neural Network selection and variable reduction, and participated in the analysis, the discussion of the data, and the writing process.
- V Participated in the definition of the research problem, proposed the initial idea of the article, proposed the use of air differential pressure sensors for underwater applications, developed the prototype, planned and conducted the experiments, designed the methodology and algorithms, analyzed the data, discussed the results, and co-wrote the article.
- VI Designed and conducted the experiments, participated in the data processing and the writing process.
- VII Proposed the use of simulated maps for localization and the initial idea of the paper, defined the research problem, planned and partially conducted the experiments, partly designed the algorithms, analyzed the data, discussed the results, and co-wrote the article.
- VIII Participated in the definition of the research problem, proposed the initial idea of the article, built the prototype, planned and participated in the experiments, designed the methodology and algorithms, analyzed the data, discussed the results, and co-wrote the article.

Abbreviations

The following abbreviations are used in this paper:

ADV	Acoustic Doppler velocimeter
ALL	Artificial lateral line
ANN	Artificial neural network
AUV	Autonomous underwater vehicle
BPF	Band-pass filter
DPSS	Differential pressure sensor system
DPSS	Differential pressure sensor speedometer
DVL	Doppler velocity log
FFT	Fast-Fourier transform
LDA	Laser Doppler anemometer
MEMS	Micro-Electro-Mechanical Systems
NACA	National Advisory Committee for Aeronautics
PIV	Particle image velocimeter
SLAM	Simultaneous Localization and Mapping
VSF	Vertical slot fishway

Symbols

g	Acceleration due to gravity (m/s^2)
h	Water depth (m)
h_0	Mean water depth in the pool (m)
h_1	Water depth upstream cross-wall (m)
h_2	Water depth downstream cross-wall (m)
TI	Turbulence intensity (%)
P	Pressure (Pa)
\bar{P}	Mean pressure (Pa)
p'	Fluctuations of pressure (Pa)
P_1	Stagnation or total pressure (Pa)
P_2	Static pressure (Pa)
psi	pressure sensor in the position i
R^2	Determination coefficient
CC	Current consumption (mA)
T	Temperature ($^{\circ}C$)
TKE	Turbulent kinetic energy ($m^2/s^2 = J/kg$)
U	Current velocity (m/s)
\bar{U}	Mean current velocity (m/s)
u'	Fluctuations of current velocity (m/s)
ΔH	Water drop (m)
ΔP	Difference in pressure (Pa)
$\Delta\bar{P}$	Mean difference in pressure (Pa)
$\Delta p'$	Fluctuations of difference in pressure (Pa)
ΔZ	Topographic difference between cross-walls (Pa)
β_{ij}	Dimensionless coefficients
ρ	Density (kg/m^3)
a	Coefficient
t	Time (s)
m	Number of particles
w	Particle weight
d	Motion step (m)
τ	Reynold stress (N/m^2)

Introduction

Multiple tools and techniques are used to sense and measure water flow and its associated hydrodynamic parameters (e.g., pressure, velocity, turbulence, etc.). However, although it is possible to use technologies which can measure in a high sampling rate and therefore correctly characterize the underwater environments under laboratory conditions, field-oriented technologies are usually associated with low sampling rates (e.g., field ADVs, propellers, rotors, etc.) [1]. In addition, field devices need to overcome the influence of obstacles, suspended particles or gas bubbles [2], [3], complex calibration processes [4], or the inefficiency involved in the measurement of low velocity flows (< 0.05 m/s) [5].

As a result of their adaptation to water habitats, fish have solved these problems with a unique sensing solution: the lateral line. The lateral lines are an array of tiny, distributed sensing organs made up of hair cells that are stimulated by the flow over the fish's body [9], allowing fish to act and react according to what they sense. Lateral lines contribute to the performance of different fish behaviors, such as rheotaxis, schooling, predator and obstacle avoidance, prey localization, as well as stationary obstacle detection to reduce energy consumption [6], [7]. The range of these natural hydrodynamic receptors can be around 200 Hz [8], which lies outside the sampling frequency of the majority of available field measuring devices.

Inspired by these natural organs, researchers have developed artificial lateral lines (ALLs). Like biological lateral lines, ALLs are usually designed as a discrete set of sensing units (sensors) placed over a body, where they record the local interaction of the fluid media with the body. There are different types of individual sensing units, and ALLs can be classified according to their sensor type [7], [9]–[13]. For instance, it is possible to find sensors with high biological similarity such as artificial hair cells that offer high sensitivities [10], [14]–[16], MEMS pressure sensors with very small dimensions [17], [18] or novel alternatives such as optical sensors [11], hot wire anemometers [19], [20] or ionic polymer–metal composites [21], [22]. However, most of the sensors listed have two major drawbacks: (1) they are too fragile to use outside laboratory conditions or (2) they are experimental sensors and, thus, not mature enough for their real application. Therefore, commodity pressure sensors are the most extended alternatives when it comes to studying the applications of ALLs, e.g., [23]–[30] among others (Section 1.1.2). Despite the lower sensitivity and the bigger sizes of pressure sensors, they allow finding supplies easily and trying different sensor alternatives according to the requirements, and their robustness is tested and validated according to standards before their commercialization.

The study of pressure sensor-based ALLs under laboratory conditions has displayed that they can approximate some of the sensing abilities of biological lateral lines such as hydrodynamic mapping [9], [13], object detection [13], flow classification [31], [32], rheotaxis [13], [33], flow-velocity estimation [13], [24] or prey detection [30], [34]. However, these devices have demonstrated satisfactory performance mainly under ideal hydrodynamic conditions [9], [13], [30], subject to intense calibration procedures [9], [27], [34] and, less frequently, their performance has depended on case specific laboratory prototypes and formulations that would be difficult to apply in real-world¹

¹ We define real-world as a not idealized condition, subject to disturbances and a large spectrum of hydrodynamic conditions, which can be compared with field-like conditions.

applications. Real-world applications, in most cases, are conducted in not idealized environments (e.g., rivers or open oceans) subject to disturbances (e.g., obstacles or waves) and large spectrum of hydrodynamic conditions (e.g., different velocities or turbulence levels). Under these conditions, calibration procedures are difficult to conduct (Section 2.3.1), and the relations established in the laboratory may not work.

To-date the use of ALLs is limited in real-world applications. Studies like [31], [35] show the potentiality of ALLs in real-world conditions by successfully discriminating between different target objects and locations with different hydrodynamic conditions. However, due to the listed limitations, these studies make use of *a-priori* feature learning process of the scenario with the ALL, making the application case specific and difficult to use in unknown environments.

Therefore, the main objective of this dissertation is to conduct a research on pressure sensor-based ALLs to provide field ready solutions, making possible their use in real-world conditions independently of the case, as well as, show the accomplishment of this objective by presenting its use in real-world applications. This is achieved by providing (1) sensor calibration independent solutions and (2) new technological alternatives to improve the overall performance of pressure sensor-based ALLs and (3) demonstrating their use in real-world applications.

Motivation

The target applications presented in the dissertation mainly fall into two categories: velocity calculation for underwater robotics and fish preference studies (*Figure 0.1*). This is the consequence of the two main projects funding this dissertation that proposed the initial idea of applying ALLs to real-world applications: BONUS Fishview project (www.bonusportal.org/fishview) and FP7 European Academy for Marine and Underwater Robotics (Robocademy project) (www.robocademy-project.eu). Nevertheless, the achievement of the thesis objective would have immediate repercussions for other applications.

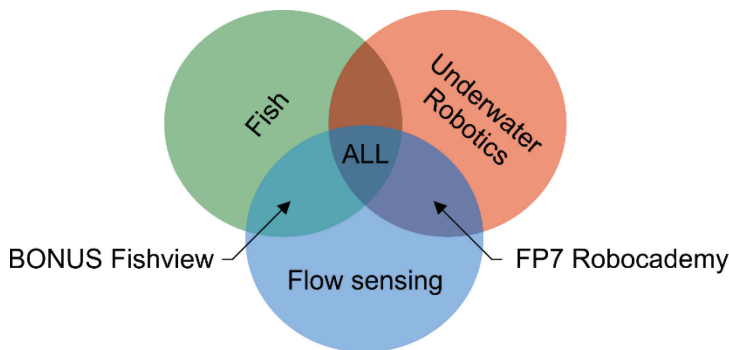


Figure 0.1. Framework of the thesis and the research conducted. FP7 Robocademy and BONUS Fishview are the projects that have funded the thesis.

ALLs have demonstrated their utility multiple times to estimate variables describing water flow (specially flow velocity) under laboratory conditions [13], [22], [26]. Furthermore, for instance in [13], [23] using pressure sensor-based ALLs vortex structures were successfully identified and tracked. This suggests that by using similar principles, a real-world ready ALL could be used to estimate other statistical variables

that further characterize not only the velocity but also the turbulence or vorticity of the fluid medium.

The application of ALLs in aquatic organism habitats and preference studies could be also immediate. Nowadays, aquatic organism habitats and preference studies make use of widely used hydrodynamic variables, such as velocity, Reynold stresses, turbulent kinetic energy, or turbulent intensity [36], and physical variables defining the environment, such as vegetation, bed composition, or water depth [37]. Considering the possibilities that could offer an ALL for hydrodynamic variable estimation [13], [22], [23], [26] as well as the identification of underwater objects and structures [31], a real-world ready ALL could offer an all in one tool for environmental monitoring, which lies outside the scope of the state-of-the-art measuring tools.

Underwater robotic sensing relies mainly on cameras and sonars [38]. Both sensing modalities might be of limited utility in certain underwater environments such as homogeneous or turbid ones. In this sense, flow sensing with ALLs could be used as a complement to perform basic underwater robotic tasks: localization by providing new exploitable features [35], [39], obstacle detection by measuring the interaction of obstacles with the flow [25], or adaptation to a specific hydrodynamic environment to optimize the drag [40], [41] and the energy expenditure [24], [42].

In the same way, velocity estimation in underwater vehicles to date relies mainly in a single technological solution, the Doppler Velocity Log (DVL). DVLs have demonstrated a good and reliable performance in many applications, e.g., [43], [44]. However, these devices are expensive, have a large size and high-energy consumption (as they consist of active sensors). This makes them unsuitable for small vehicles [45], [46] or situations requiring low-energy consumption [47]. In contrast, pressure sensors are passive, which reduces their power consumption, and smaller, which has already allowed the installation of pressure sensor-based ALLs in small laboratory robotic platforms [25], [48]. Consequently, an ALL ready to be used in different field cases and able to provide real-time measurements could cover the technological gaps described above and, consequently, stimulate the development of small vehicles or increase the reliability and precision of vehicles oriented toward prolonged missions.

Problem statement and methodological approach

Consequently, the general problem statement of this dissertation is as follows:

Our aim is to use pressure sensor-based ALLs in laboratory and real-world applications, specifically in underwater robotics and underwater environment studies.

However, so far pressure sensor-based ALLs have only demonstrated satisfactory performance under ideal hydrodynamic conditions. Their use is limited in real-world applications due to the calibration procedures and the large spectrum of possible hydrodynamic conditions, and, frequently, their performance has been demonstrated using laboratory designs difficult to apply in real-world conditions.

To achieve our aim, we will use an experimental approach to study possible alternatives for hydrodynamic variable estimation independent of calibration procedures and under different spectra of hydrodynamic conditions. This will allow us to propose solutions as well as to drive conclusions of the applicability and limitations of the state-of-the-art pressure sensor-based ALLs (absolute pressure

sensor-based ALLs). Considering the encountered limitations, we will develop a new method to use differential pressure sensors in ALLs, which will increase their sensitivity, effective sampling frequency,² and applicability in real-world conditions. This will be demonstrated using the proposed solution under real-world applications.

Figure 0.2 illustrates the general 3-step path conducted to fulfill the aim of the dissertation as well as its organization. The path followed has been a result of the findings in each of the researching steps, therefore it follows an incremental development. However, each specific step has followed an iterative process.

Flow sensing with pressure sensor-based artificial lateral lines:
from the laboratory to the field

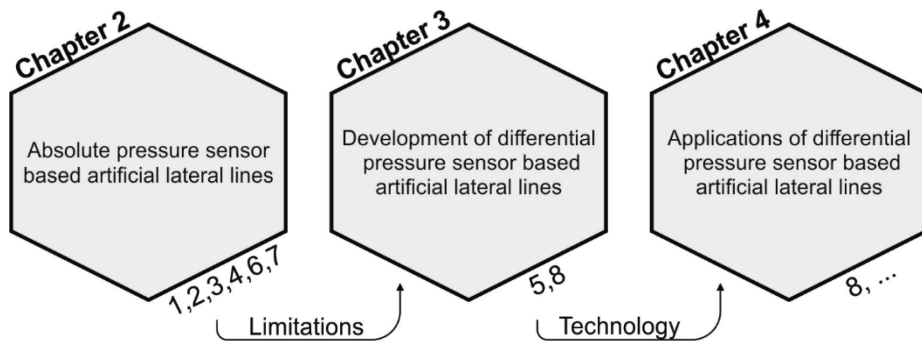


Figure 0.2. Path followed in the dissertation, organization of the dissertation and article relation. Numbers in the hexagons refer to the papers.

First, the research was focused on the evaluation of the performance and usefulness of the current state-of-the-art absolute pressure sensor-based ALLs (Figure 0.3). For this a prototype that gathers all the advances made in the Centre for Biorobotics, Tallinn University of Technology (Estonia) in ALLs [24], [25] was used (Figure 0.4). This prototype was subject to experimental setups with a wide spectrum of hydrodynamic conditions. As a result of the research, in contrast to previous studies, e.g., [13], [22], [26], novel algorithms and relations to estimate hydrodynamic variables (not only velocity but also turbulence), in diverse hydrodynamic conditions, independent of sensor calibration procedures and angular distortions were developed. The methods applied are derived from statistical approaches, exploring different flow pressure features, to neural network approaches that exploit the distributed sensing capabilities of the ALL (cf. Chapter 2).

² Sampling frequency at what ALLs can provide valuable data.

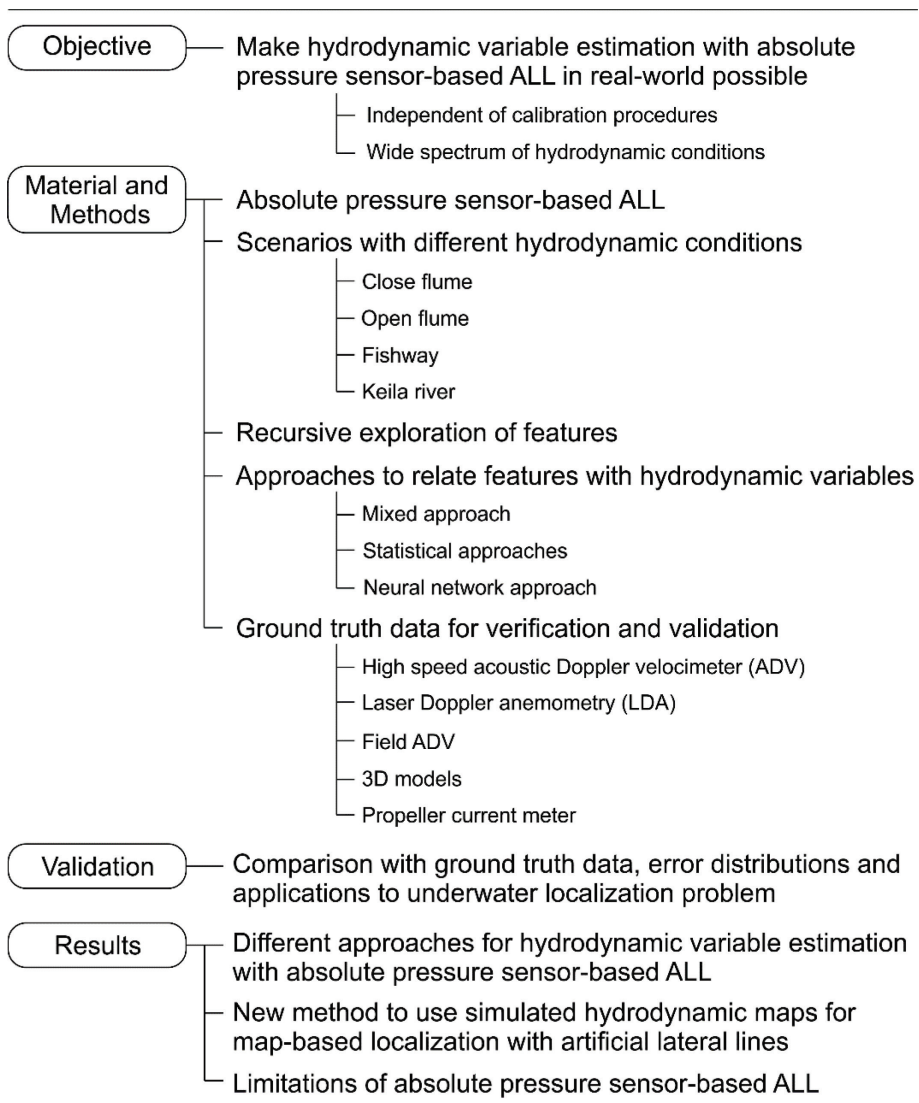


Figure 0.3. Summary of first step (Chapter 2) of the present dissertation.



Figure 0.4. Some of the studied scenarios with the absolute pressure sensor-based ALL. a) Open flume. b) Fishway. c) Keila river (Estonia).

In addition, using the developed relations and as an example of their applicability, a new method to use simulated hydrodynamic maps for map-based localization is proposed. This approach, advance in the algorithms proposed in [35] by providing an alternative to perform localization using flow features without the need of scenario learning or feature pre-calibration procedures.

Despite the advances made in the absolute pressure sensor-based ALLs, the main conclusions driven from their research in the first step show that for most applications these devices will need to be subject to intensive feature learning and training procedures to derive quality results and that their application for real-time applications is very limited (Results, *Figure 0.3*).

Therefore, once the limitations were identified, an alternative research and analysis was conducted to try to solve them. As a result, a novel method for using air differential pressure sensors in ALLs was developed (cf. Chapter 3) (*Figure 0.5*). This method can bypass the technological limitations and constraints offered by commodity absolute pressure sensors (e.g., calibration, depth dependent sensitivity, or atmospheric influence) as well as available wet-to-wet differential pressure sensors (e.g., form factor, cost, or sensitivity). In addition, a new general relation capable of providing accurate instantaneous estimates of velocity independent of the angle of attack was determined. By doing so the main drawbacks identified in the previous absolute-pressure sensor ALLs, e.g., [31], [49]–[51], were solved.

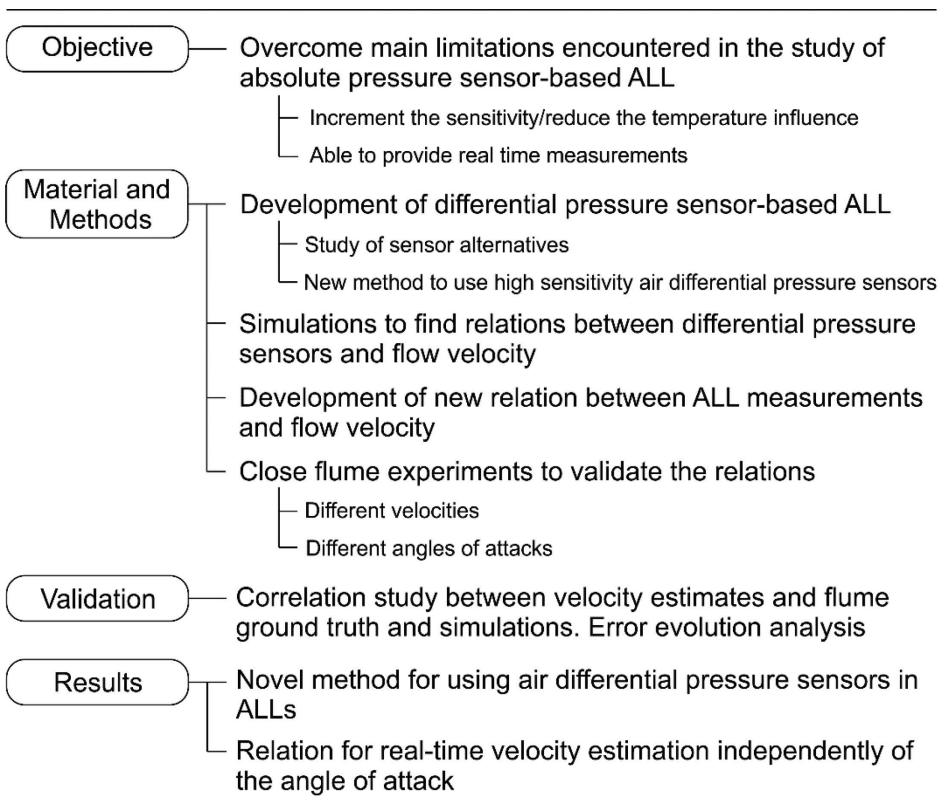


Figure 0.5. Summary of second step (Chapter 3) of the present dissertation.

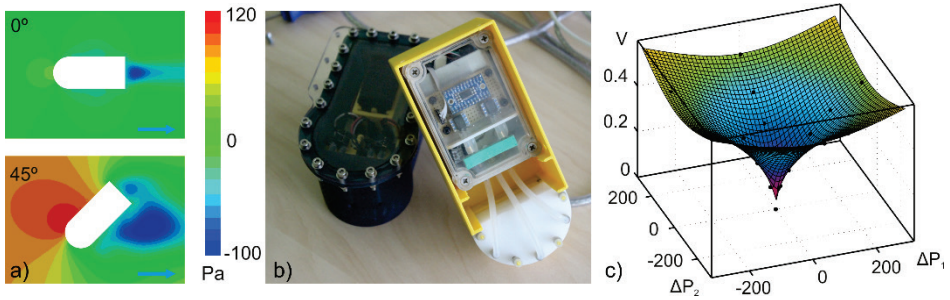


Figure 0.6. Some results from the experimental study conducted in the second step. a) Part of the simulations. b) First prototype developed. c) Relation between velocity and differential pressure.

To demonstrate the utility of the new technology developed under real-world application, two test cases were considered: velocity estimation for underwater applications and fish preference studies. Accordingly, two tools were developed: Differential Pressure Speedometry System (DPSS), an artificial lateral line designed for velocity estimation in torpedo-shaped underwater robots, and iRon, the first differential pressure sensor-based ALL for environmental monitoring (Figure 0.7).

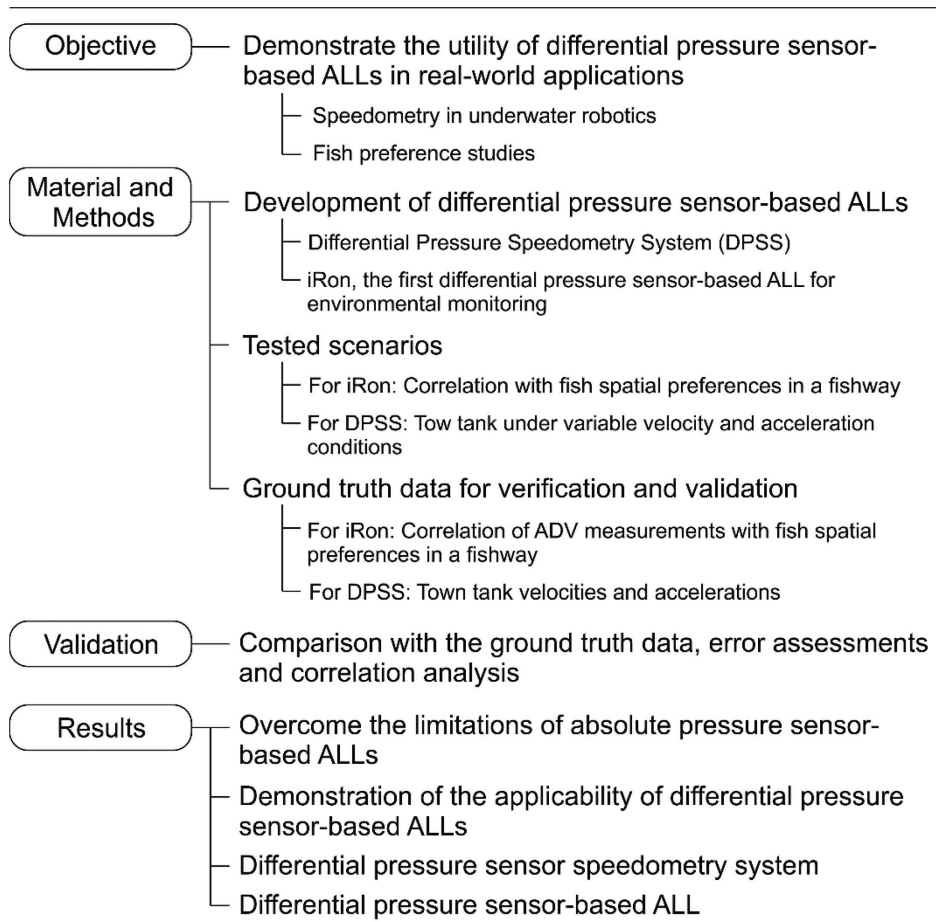


Figure 0.7. Summary of third step (Chapter 4) of the present dissertation.

The tests conducted with the DPSS and iRon (Figure 0.8) were compared with their respective ground truth datasets (Figure 0.7) to show their performance and applicability and to confirm that differential pressure sensor-based ALLs could overcome the limitations of absolute pressure sensor-based ALLs.

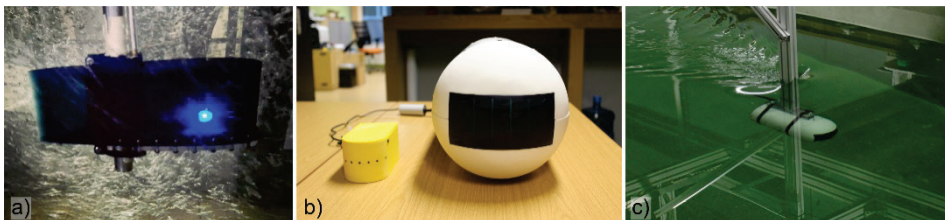


Figure 0.8. Illustration of the applications studied in third step. a) iRon subject to turbulent bubbly flow in a fishway. b) Dimension comparison of the DPSS and the first prototype developed. c) DPSS in the tow tank.

Specific contributions of the thesis

This thesis contributes to the development of artificial lateral lines and its real-world applications by:

- Experimentally determining novel algorithms and relations to estimate hydrodynamic variables (velocity and turbulence) from absolute pressure sensor-based artificial lateral lines independent of calibration procedures and angular distortions.
- Developing a new method to use simulated hydrodynamic maps for map-based localization with artificial lateral lines.
- Showing that the limitations of absolute pressure sensor-based lateral lines made them unpractical for some real-world applications (e.g., real time applications or intense testing procedures).
- Proposing and developing a novel method for using air differential pressure sensors in artificial lateral lines.
- Experimentally determining a general relation between differential pressure sensor-based artificial lateral lines output and velocity, capable of providing accurate instantaneous estimates of velocity independently of the angle of attack of the body where the lateral line is installed on.
- Designing and building artificial lateral line platforms for velocity estimation in underwater robots and for environmental monitoring.
- Demonstrating that differential pressure sensor-based artificial lateral lines overcome the main limitations detected in absolute pressure sensor-based artificial lateral lines, which makes possible their use in the target real-world applications (i.e. underwater velocity estimation and fish preference studies).

Outline of the thesis

The results of the dissertation are divided into four chapters:

Chapter 1 provides general background, an overview of ALLs research, defines the main concepts used along the thesis. By doing so the scientific context of the thesis is defined.

Chapter 2 summarizes the conducted research using state-of-the-art absolute pressure sensor-based ALL. Classical approaches are analyzed as well as new methods are proposed to deal with real-world conditions and to perform time-averaged flow velocity and turbulence variable estimation. As an application example, one of the proposed new methods is used to solve a map-based localization problem using simulated hydrodynamic maps. The chapter concludes that the limitations encountered in absolute pressure sensor-based ALLs may limit their application in many real-world applications. Articles: 1, 2, 3, 4, 6, 7.

Chapter 3 attempts to overcome the limitations of absolute pressure sensor-based ALLs by proposing a novel engineering method to employ air differential pressure sensors in the design of ALLs. A new prototype is developed, and its performance is studied, modeled and validated. By the study of the prototype, a simple empirical relation able to provide accurate real-time velocity is defined. Articles: 5, 8.

Chapter 4 deals with the real-world applications tested with differential pressure sensor-based ALLs. Particularly, it is shown that using the results from the previous steps of the dissertation, the developed technological results can be applied in underwater robotics to estimate the velocity and in environmental monitoring applications for fish preference studies. Article: 8 and results submitted for publication.

1. General background

The aim of this thesis is to make feasible the use of artificial lateral lines (ALLs) in environmental studies as well as underwater robotics, under laboratory and real-world applications. Consequently, it is a multidisciplinary work (*Figure 0.1*) at the frontier of robotics, bioinspired flow sensing, ecology and hydraulics. Therefore, it is necessary to describe a general background to familiarize readers from different areas to the main topic, artificial lateral lines, and to define the scientific context of the thesis.

To achieve this, the following chapter provides an overview of ALLs. The main concepts used along the thesis are defined and previous and ongoing research is summarized and classified. To place the thesis in the ALLs research context and give a recent overview of the research performed so far, publications from the thesis have also been included in this review.

1.1. Artificial lateral lines

Aquatic vertebrates have evolved in water and due to this reason many can sense the water's hydrodynamic characteristics. One of the most important adaptations in sensing is the lateral line (*Figure 1.1*).

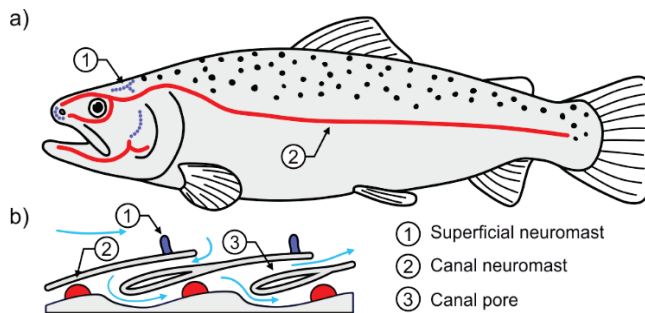


Figure 1.1. Lateral line system [1]. a) Distribution of neuromasts. b) Superficial and canal neuromasts.

The lateral line is partially responsible for various common behaviors in fish, such as prey and predator detection [52], [53], obstacle avoidance [54], rheotaxis [55] or schooling [56], among others.

This sensing organ consists of an array of mechanoreceptors, neuromasts, each capable of sensing local mechanical changes in water [52], [57] (*Figure 1.1*). These neuromasts consist of a group of hair cells covered by a jelly-like substance. Together, these hair cell bundles form a cupula, providing fish a linkage with the environment [57]. The movement of the cupula causes the deflection of the hair cells, and this is translated into a stimulus. Depending on the neuromast distribution, in an array within a canal or alone in the surface (*Figure 1.1.b*), their structure and perceptions differ slightly. The former are more sensitive to pressure gradients, while the latter are directly affected by near-body accelerations and velocity gradients [58].

The efficiency and utility of this organ under different complex environmental conditions, such as turbulent flow, turbidity or darkness, has inspired human beings to develop their artificial analogous: the artificial lateral line [7], [9], [11], [12], [20], [59].

The potential functionalities of ALLs would have immediate applications in diverse underwater fields.

For instance, in underwater robotics ALLs could offer a new sensing alternative for performing basic tasks such as localization [35], [39], obstacle and wall detection [25], [60], [61], vehicle velocity estimation [62] or more advance tasks such as energy expenditure and drag reduction [40], [63].

Similarly, it would also provide an excellent opportunity for ecological studies, as due to its distributed sensing capability, in contrast to other field hydrodynamic measuring devices, ALLs have the potential to evaluate biologically relevant data with a higher dimensionality [32], [64].

1.1.1. Types of ALLs

All the ALLs developed by different researcher groups are based on the same design principle. The simplest unit, the neuromast, is substituted by an artificial sensing unit that can measure the local interaction of the fluid with the body (e.g., artificial hair cells [10], hot wire elements [19], pressure sensors [13], [65], ionic polymer-metal composites [21] or optical sensors [11]) (*Table 1.1 and Figure 1.2*).

Table 1.1. Sensing units used to elaborate artificial lateral lines.

Type	Year ¹	Ref. ²	Applications and observations
Artificial hair cells	2002	[59]	<ul style="list-style-type: none"> • Only tested in idealized laboratory conditions • High sensitivity • Small dimension • Customizable • Fragile, limited durability • Hardly accessible • Few types
Hot wire elements	2006	[20]	<ul style="list-style-type: none"> • Only tested in idealized laboratory conditions • High sensitivity • Small dimension • Customizable • Fragile • Hardly accessible • Few types
Ionic polymer-metal composites	2011	[21]	<ul style="list-style-type: none"> • Only tested in idealized laboratory conditions • High sensitivity • Medium/big dimensions • Customizable • Fragile, limited durability • Fairly accessible but challenging implementation • Few types
Optical sensors	2011	[11]	<ul style="list-style-type: none"> • Only tested in idealized laboratory conditions • High sensitivity • Medium/big dimension • Partly customizable • Fragile • Easily accessible sensor unit but challenging implementation • Multiple types
Commercial pressure sensors	2011	[23], [26]	<ul style="list-style-type: none"> • Tested in multiple laboratory conditions and field applications³ • Low sensitivity • Medium/big dimension • Not customizable • Robust • Easy implementation • Easily accessible • Multiple types

¹Year of the 1st reference.

²First reference proposing the target sensing unit for its use in ALLs to the best of the knowledge of the author of the thesis.

³The present thesis has contributed to achieve this.

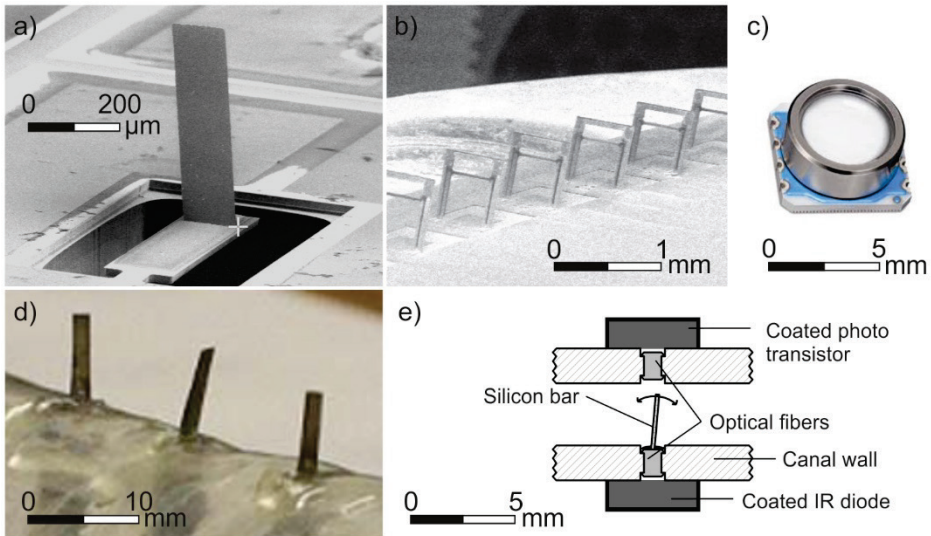


Figure 1.2. Examples of sensing units used to elaborate artificial lateral lines. a) Artificial hair cells (modified from [59]). b) Hot wire elements (modified from [20], © 2006 National Academy of Sciences). c) Absolute pressure sensor MS5540C [66]. d) Ionic polymer-metal composites (modified from [21], © 2011 IEEE). e) Sensing unit based in optical sensors (modified from [11]).

Table 1.1 summarizes the different sensor types that have been proposed and used to elaborate ALLs as well as their principal characteristics and limitations. Despite the extensive research on ALLs, satisfactory performance has mainly been obtained under idealized conditions [7], [9], [13], [19], [20], that is to say conditions without disturbances (laboratory) and controlled hydrodynamic variables (controlled velocity, turbulence level and fixed depths) (Table 1.1). In the same way, frequently the studied prototypes have not been mature enough to translate into real-world or field applications, e.g., [12], [14], [19], [59].

The most extended sensor alternative to elaborate ALLs are pressure sensors (Section 1.1.2). The main drawback of pressure sensors are their bigger dimensions and lower customization and sensitivities when compared with some experimental alternatives such as artificial hair cells or hot wire elements (Table 1.1). However, due to their use in industrial applications they are accessible, it is easy to find supplies and their robustness is tested according to standards. These characteristics make them ideal candidates to elaborate field-oriented prototypes as a field prototype should be reliable and robust to provide replicable data over time.

1.1.2. Absolute and gauge pressure sensor-based ALLs

Pressure sensor-based ALLs record the interaction of the fluid with the body in terms of pressure (or current), mimicking the performance of biological lateral lines in a simplified manner [67]. They are extensively used due to: (1) the facility of finding supplies and switching between different sensors according to the requirements of a particular setup, (2) their reliability, (3) their short development-testing cycle, (4) the direct relation of pressure with flow properties (Section 1.2.1), (5) their tested performance in other underwater applications (e.g., depth measuring), and (6) their cost.

Presently, the most popular commercial sensing unit used to build ALLs are piezo resistive transducers or pressure sensors. Specifically, absolute pressure sensors or gauge pressure sensors (*Table 1.2*).

Table 1.2. Summary of existing ALL with absolute or gauge pressure sensors, ordered with regard to prototype and researching groups.

Ref.	Year ¹	Sensor	Max Pressure	Type	Applications and observations
[23], [28]	2011	Honeywell 19C015PG4K	104 kPa	Gauge	<ul style="list-style-type: none"> • Fixed platform for the detection of a moving cylinder in laboratory conditions • Vortex tracking in a laboratory setup
		Honeywell 242PC15M	104 kPa	Gauge	<ul style="list-style-type: none"> • Fixed platform to detect the shape of a moving cylinder in laboratory conditions
[9], [13], [26], [31], [33], [63]	2011	Measurement Specialties MS5407-AM	700 kPa	Abs.	<ul style="list-style-type: none"> • Tail beat selection according to flow velocity in a fixed fish robotic platform in a laboratory setup • Braitenberg controller for a fish robot in laboratory conditions • Kármán vortex street detection fixed platform in a laboratory setup • Flow-relative and flow-aided navigation of a biomimetic underwater vehicle in laboratory conditions • Flow feature extractions for localization in field environments
[38]	2012	Freescale MPXV7007	7 kPa	Gauge	<ul style="list-style-type: none"> • Yaw control in a fixed platform in a laboratory setup
[9], [29], [65]	2013	Measurement Specialties MS5401-AM	100 kPa	Abs.	<ul style="list-style-type: none"> • Study of self-motion effect in hydrodynamic signals in a fixed laboratory robotic platform
[27], [30], [48]	2015	Consensic CPS131	120KPa	Abs.	<ul style="list-style-type: none"> • Velocity estimation for a robotic fish under laboratory conditions • Detection of the beating frequency and distance of a neighbor-fixed robotic laboratory platform • Evaluation of velocity estimation in a freely swimming robotic platform in laboratory conditions

Table 1.3. (cont.) Summary of existing ALL with absolute or gauge pressure sensors, ordered with regard to prototype and researching groups.

Ref.	Year ¹	Sensor	Max Pressure	Type	Applications and observations
[1], [32], [35], [39], [49]–[51], [64], [68], [69]	2015	Silicon Microstructures SM5420C-030-A-P-S	207kPa	Abs.	<ul style="list-style-type: none"> • One of the prototypes used in this thesis • Various methods for flow velocity and turbulence estimation under different hydrodynamic scenarios • Map-based localization methods offline using flow • Hydrodynamic signature classification under field conditions
[34]	2017	Measurement Specialties MS5803-01BA	100 kPa	Abs.	<ul style="list-style-type: none"> • Kármán vortex street detection with a fixed robotic platform in a laboratory setup
[70]	2017	Measurement Specialties MS5803-02BA	200 kPa	Abs.	<ul style="list-style-type: none"> • Velocity estimation for a robotic fish under laboratory conditions • Robot orientation under constant flow velocity in laboratory
[71], [72]	2017	Freescale MPXV5004GC6 U	3.92 kPa	Gauge	<ul style="list-style-type: none"> • Dipole source localization in laboratory conditions
[73]	2018	Measurement Specialties MS5803-07BA	700kPa	Abs.	<ul style="list-style-type: none"> • Flow velocity estimation under laboratory conditions

¹Year of the 1st reference

Absolute pressure sensors (*Figure 1.3.a*) measure pressure in reference to a space with zero pressure (vacuum); therefore, they can measure pressures from zero (i.e., lower than atmospheric pressure). While, gauge pressure sensors (*Figure 1.3.b*) measure the pressure relative to the value of the ambient atmospheric pressure (or a reference pressure if they are not directly connected to the ambient atmosphere).

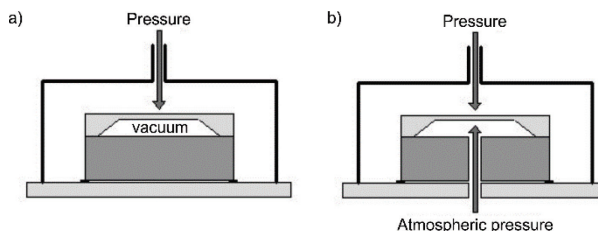
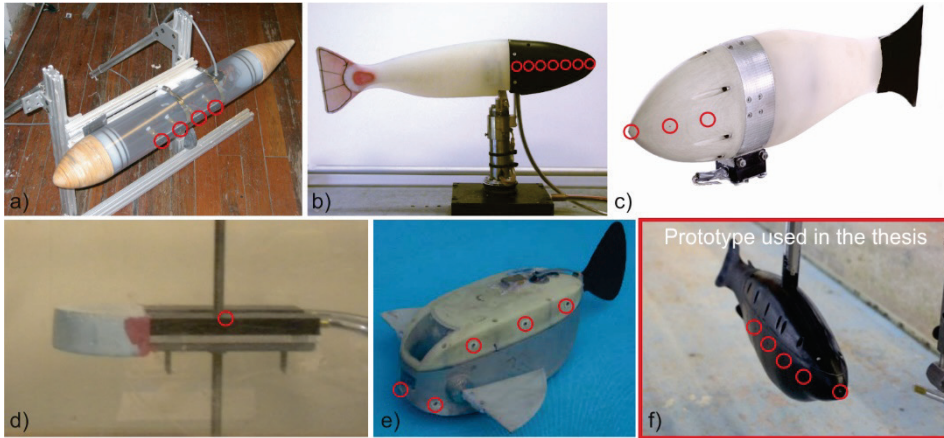


Figure 1.3. Difference between (a) absolute and (b) gauge (modified from [74]).

When these sensors are used for underwater applications, it is necessary to consider that the water column above the sensor will generate a pressure source that will also be

measured by the sensor. The deeper the application, the higher will be the pressure ranges to be used. This will have a direct impact on the sensitivity.

Once the pressure sensor type is selected, sensors are distributed in an array over the target body/prototype to create the ALL (*Figure 1.4*). Due to the diversity of possible body shapes, there is no general design principle to select the sensors' positions. However it may be selected from the preliminary study of the interaction of the specific shape with the fluid media [62], [73]. Considering the specialized references, it is a common design principle to situate one of the sensors in the front part (point facing directly the flow, stagnation point) and the others uniformly distributed (in most of the cases in the middle line of the body).



○ Position of pressure sensor

Figure 1.4. Examples of prototypes with absolute and gauge pressure-sensors based ALLs installed (position of sensor in red). a) [23]. b) [24]. c) [25]. d) [9]. e) [48], © 2015 IEEE. f) The absolute pressure sensor-based ALL studied in the present dissertation.

1.1.3. Differential pressure sensor-based ALLs

One of the contributions of this thesis is to propose and use differential pressure sensors to develop ALLs (*Figure 1.5.a*) in order to overcome many of the drawbacks associated with absolute and gauge pressure sensor-based ALLs (Chapter 2). Differential pressure sensors have been widely used in many engineering fields [75], [76], to measure the relative velocity (*Figure 1.5.b*), angle of attack, yaw rate or altitude of aircrafts [77]–[80], estimate the flow in pipes, for physical modeling studies, wind or flow tunnels, among others.

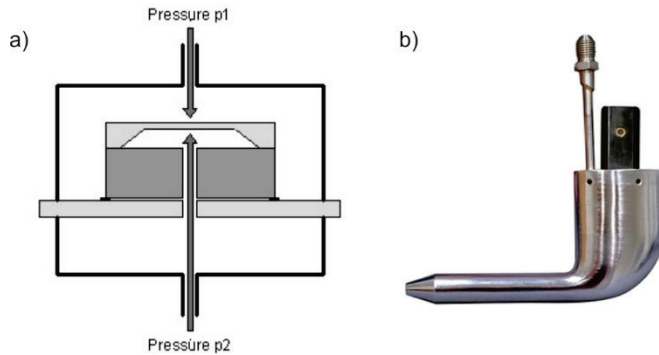


Figure 1.5. a) Working principle of differential pressure sensors (modified from [74]). b) aircraft Pitot tube [81].

Differential pressure sensors operate in a manner similar to gauge pressure sensors (Section 1.1.2), but instead of using ambient atmospheric pressure for reference, they employ another point of the medium under study. This conceptual change seems insignificant; however, by doing so in underwater applications it is possible to compensate the pressure due to the water column above the sensor between ports. This means that it is possible to increase the sensitivity exponentially, measuring only the dynamic component of the pressure (i.e., change of pressure due to the interaction of the body with the flow) and be independent of the application depth.

Considering the previous examples (Table 1.2) and comparing them with one of the differential pressure sensors used in this thesis (Table 1.4), we could shift from a pressure range of 207 kPa (Silicon Microstructures SM5420C-030-A-P-S) to 2 kPa (NXP Semiconductors MPXV7002), i.e., a sensitivity increment of 10000%. Additionally, the need of lower pressure ranges implies lower noise ratios as well as better stability in comparison to error sources such as temperature.

To the best of our knowledge, they are only two research groups working on differential pressure sensor-based ALLs (Table 1.4): the research group in Thermal Sciences and Fluid Dynamics of University of Florida and Centre for Biorobotics of Tallinn University of Technology.

Table 1.4. Summary of differential pressure sensor-based ALLs with differential pressure sensors, ordered by researching group and sensor type.

Ref.	Year ¹	Sensor	Max Pressure	Applications and observations
[62], [82]– [87]	2016	Honeywell SSCDRRN005ND2A5	± 1244 Pa	<ul style="list-style-type: none"> • Prototypes developed in the framework of this thesis (B-Box 2015) • Proof of the concept of differential pressure based ALL for flow velocity estimation • Tested under laboratory conditions
		NXP Semiconductors MPXV5004	0-3920 Pa	<ul style="list-style-type: none"> • Prototypes developed in the framework of this thesis (D-Box 2016) • Prototype developed for turbulence estimation in hydropower plants • Tested under field conditions
		NXP Semiconductors MPXV7002	± 2000 Pa	<ul style="list-style-type: none"> • Prototypes developed in the framework of this thesis (DPSS 2017) • Developed for instantaneous flow velocity estimation in underwater vehicles, • Tested under field and laboratory conditions
		NXP Semiconductors MPXV7002	± 2000 Pa	<ul style="list-style-type: none"> • Prototypes developed in the framework of this thesis (iRon 2016) • Analysis of fish preferences and behaviors • Tested under field and laboratory conditions
[60], [61], [88]	2016	NXP Semiconductors MPXV7002	± 2000 Pa	<ul style="list-style-type: none"> • Force estimation and wall detection • Tested under laboratory conditions

¹Year of the 1st reference

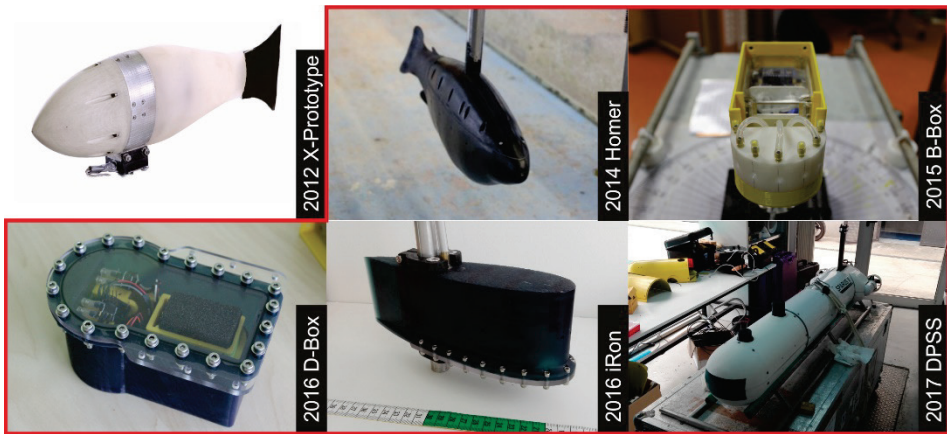


Figure 1.6. Evolution of the ALL technology in the Centre for Biorobotics; From final results of the EU project FILOSE (231495) to the progress made during this thesis (in red).

1.2. Applications of ALLs

The summary tables presented in the previous sections (*Table 1.2 and Table 1.4*) list the applications conducted with pressure sensor-based ALLs. These applications mainly focus on sensing and characterizing underwater media and, less frequently, in the use of this information to perform more advanced tasks such as the control of underwater vehicles or environmental studies.

Sensing applications can be classified into two different categories: (1) hydrodynamic mapping and (2) hydrodynamic sensing. In *hydrodynamic mapping applications*, applications that aim to determine spatial information from ALL output can be included, such as dipole source localization [7], [11], [14], [17], [19]–[21], [89] (*Figure 1.7.a*), which consists of situating a stimuli source in space, the characterization of a Kármán vortex street generated behind an obstacle [9], [11], [14], [20], [29], [30] (*Figure 1.7.b*) or the identification of object velocities and shapes passing over the ALL [23]. These tasks, in the majority of the cases, have been conducted with static ALLs and evaluated using ideal laboratory setups, i.e., environments with the absence or flow hydrodynamic disturbances.

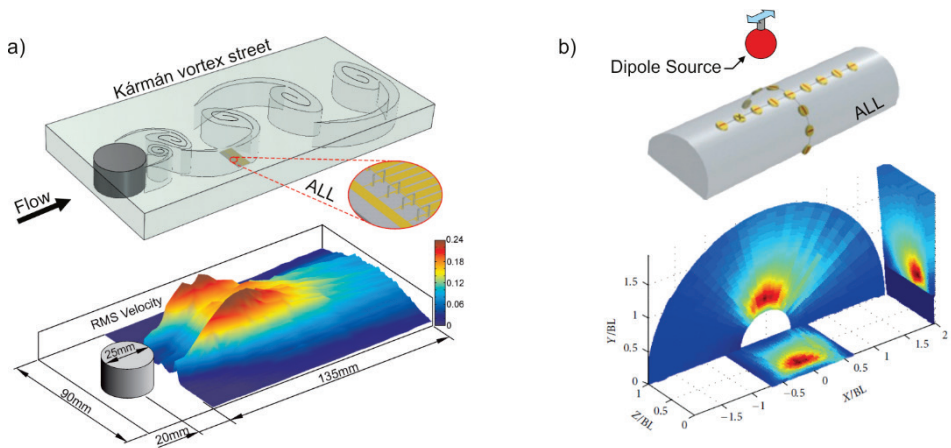


Figure 1.7. Examples of hydrodynamic mapping using ALLs. a) Mapping of vortex signatures using hot wire element based ALL (modified from [20], © 2006 National Academy of Sciences). b) 3D localization of a dipole source using artificial hair cells based ALL (modified from [90]).

Under the *hydrodynamic sensing* category, it is possible to include any task with the aim to characterize flow properties or its hydrodynamic characteristics (e.g., flow velocity, turbulence, vorticity, etc.). Multiple studies have proposed approaches to infer flow velocity from ALLs readings [13], [26], [27], [49]–[51], [65], [82], [91] as well as turbulence [49], [50].

Both sensing applications can be directly used in the control of underwater vehicles or in the characterization of fluid media for environmental studies; however, few researching works have achieved these types of applications.

The first advances in control and navigation of underwater vehicles with ALLs were accomplished by the FP7 FILOSE European project. In this project, the team successfully imitated rheotaxis, station-holding behaviors, and flow direction detection using a robotic fish [13], [33]. Later, members of the Intelligent Control Laboratory of Peking University also demonstrated the possibility of velocity estimation with a freely swimming robotic fish in steady conditions [48], [92]. Nevertheless, all these cases were performed under controlled conditions using laboratory prototypes with absolute pressure sensor-based ALLs.

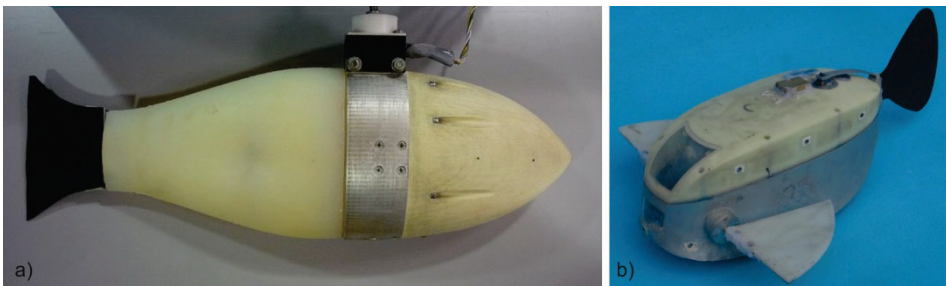


Figure 1.8. Two examples of robotic fish with artificial lateral lines. a) Filose robot (Author: Jaan Rebane). b) Robotic fish developed by Intelligent Control Laboratory of Peking University (modified from [48], © 2015 IEEE).

Regarding environmental monitoring or characterization, only one international project has attempted to use ALLs for this purpose: the BONUS Fishview project (2014–2017). This project motivated part of the results and developments of the present thesis. The notion behind the use of ALLs for environmental monitoring is that their sensing capabilities are closer to the fish’s perspective as compared with common techniques used for the measurement flow hydrodynamic characteristics (e.g., ADV, propellers, etc.). Therefore, the features obtained with these devices could represent the fish’s preferences better. Today, the exploration of ALLs for environmental monitoring continues under the FIThydro H2020 project (2016–2020).

Despite the potential usage of ALLs, their application have been mainly laboratory oriented, and it was not until 2015 when the first results under field applications were reported [31], [32]. To the best of our knowledge, the Centre for Biorobotics has been the only research group taking this step.

One of the main problems of using absolute pressure sensor-based ALLs under field applications is the need of pressure sensor calibration prior to and subsequent to each use [9], [27], [34]. This is motivated by their reduced sensitivity, their working principle and design characteristics, which increase their sensitivity to environmental disturbances (e.g., temperature and water level changes or atmospheric pressure oscillations) (discussed more deeply in Chapter 2). This thesis overcomes these limitations by proposing techniques which can support high environmental disturbance levels and eliminate the pressure sensor calibration before each experiment from the workflow (Chapter 2). This allows the measurement of hydrodynamic variables with ALLs under different environmental conditions.

In the same way, a novel method to use differential pressure sensors to design ALLs is proposed (Chapter 3). By using differential pressure sensors to design ALLs, it is possible to overcome many of the limitations encountered in the use of absolute pressure sensor-based ALLs. For instance, contrary to the proposed techniques with absolute pressure sensor-based ALLs, they allow real time water velocity estimation. This allowed us to extend the applicability of ALLs in field and real-world conditions (Chapter 4).

1.2.1. Hydrodynamic variable estimation using pressure sensing

Considering the applications listed in *Table 1.2*, flow velocity estimation is one of the most extended benchmark tests of pressure sensor-based ALLs [13], [24], [26], [27], [48], [73]. This is due to the importance of velocity for underwater vehicle control (which is a common target application of ALLs research) [26], [48], [93], the relation of hydrodynamic variables with ecological and biological processes [36], [85], and the direct relation of pressure with flow velocity [16], [17].

Bernoulli’s law [94] describes the fundamental relation between pressure (P) and fluid flow velocity (U) for an inviscid, incompressible flow:

$$P + \frac{1}{2} \rho U^2 = \text{constant} \quad (1)$$

where P is the fluid’s hydrostatic pressure (Pa), ρ is the density (kg/m³), and U is the fluid flow velocity (m/s). The law states that between two points along the same streamline, the relation between U and P remains constant.

A direct application of this principle, assuming irrotational and steady flow, is the velocity estimation achieved through the measurement of the pressure difference across

two points of a submerged body [75], [95], [96]. Considering Eq. (1) and ideally a point in the stagnation position (P_1), the point with maximal pressure and a velocity equal to zero, and a second point subject to the freestream velocity (P_2), the following equation is given (Pitot relation):

$$P_1 = P_2 + \frac{1}{2} \rho U^2 \rightarrow \Delta P_{1,2} = P_1 - P_2 = \frac{1}{2} \rho U^2 \rightarrow U = \sqrt{\frac{2 \cdot \beta_U \cdot \Delta P_{1,2}}{\rho}} \quad (2)$$

where $\Delta P_{1,2}$ is the difference in pressure between the point 1 and the point 2 (Pa). This comprises the most commonly employed method to estimate velocity in pressure sensor based ALL studies [13], [24], [26], [27], [65]; however, despite the fact that it is easy to identify the stagnation point (i.e., the point facing the flow), in practice, the point whose velocity is equal to the freestream velocity will move according to the body shape. To resolve this issue, for instance, [13] introduces a semi-empirical correction factor that multiplies $\Delta P_{1,2}$ (β_U) in the Eq. (2). This factor will depend on the pressure sensor position used to measure P_2 as well as the geometry of the body.

If U is estimated fast, later it is possible to decompose it into two components by means of Reynolds decomposition into a time-averaged component (\bar{U}) and its fluctuations (u'). Fluctuations could be used to further characterize the flow through the calculation of the turbulence metrics.

The relation between flow velocity and pressure is the conventional way to estimate flow velocity or the vehicle velocity, either using empirical relations [13], [26], [70] or Eq. (2) [13], [24], [26], [27], [65]. Although this relation has demonstrated accurate estimates under controlled environments, absolute and gauge pressure sensor-based ALL limitations will make it difficult to apply it in real-world applications (Chapter 2).

1.3. Summary and conclusions

From this chapter it can be concluded that the complexity of real-world conditions has limited the applicability of absolute pressure sensor-based ALLs to laboratory setups and ideal hydrodynamic conditions. However, the main motivation of this research has always been to use ALLs in real-world applications. The methodological approaches and technologies developed for the laboratory are substantially different than the ones developed for field or real-world applications. Real-world conditions are characterized by their hardness and dynamism. Therefore, the proposed solutions must consider these constraints. This thesis has contributed to the application of ALLs in the real-world by proposing new methods to use the classical absolute pressure sensor-based ALLs (Chapter 2), improving the pressure-based ALLs by making possible the use of differential pressure sensors (Chapter 3), and demonstrating their possible application (Chapter 4).

2. Flow sensing with absolute pressure sensor-based ALLs

In this chapter, we study the performance of absolute pressure sensor-based ALLs focusing on the estimation of flow hydrodynamic parameters (flow velocity and turbulence metrics). First, the classical approach based on Bernoulli's principle is applied and evaluated to identify the main factors which limit its applicability under real-world conditions. Next, new approaches capable of being used in real-world conditions are proposed; these approaches are (1) independent of sensor calibration procedures before every new use and (2) able to handle a wide spectrum of hydrodynamic conditions.

1. *Classical approach* (article: 1): solution based on Bernoulli's principle (Section 2.3.1).
2. *Mixed approach* (article: 1): solution that combines a 2-step procedure including a statistical approach with Bernoulli's principle (Section 2.3.2).
3. *Statistical approach* (articles: 2 and 6): purely statistical approaches not related to Bernoulli's principle (Section 2.3.3).
4. *Neural network approach* (article: 4): makes use of a neural network together with the cross-correlation between sensors (Section 2.3.4).

To study and test the different approaches, an absolute pressure sensor-based ALL is used (Section 2.1) and 4 different scenarios with different hydrodynamic characteristics are studied (Section 2.2).

The chapter ends with an application of the proposed approaches in a map-based localization problem, which illustrates one possible application of the findings (Section 2.4).

2.1. The studied prototype

The absolute pressure sensor-based ALL used for this study is a prototype that gathers all the advances made in the Centre for Biorobotics, Tallinn University of Technology (Estonia) in this area during the last few years [24], [25]. This ALL has been installed in an acrylonitrile butadiene styrene (ABS) plastic cover of 0.45 m length in the shape of an adult, farm-raised, rainbow trout (*Oncorhynchus mykiss*). The ALL consists of 16 pressure sensors with full sensitivity in a 0–207 kPa range (SM5420C-030-A-P-S) and two 3-axis accelerometers (ADXL325BCPZ) (Figure 2.1).

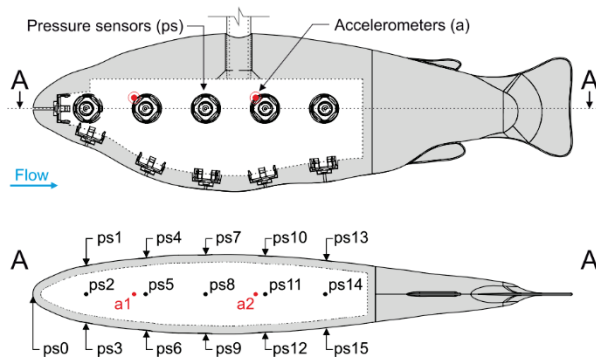


Figure 2.1. Distribution of the pressure sensors in the prototype used in the present study; ps0 is the nose sensor, and ps1 to ps15 are the lateral sensors [50].

Due to the different configurations of each scenario, different experimental procedures have been employed for each one. *The closed flume* (Figure 2.2.a) consists of a rectangular flume with a closed working area of 0.5 m x 0.5 m x 1.5 m. It has a motor that induces the recirculation of the water, and the discharge is redistributed over the tunnel cross section before entering the working area by means of two collimators. The flume can generate flow velocities ranging from 0.05 to 0.5 m/s with an accuracy of 0.04 m/s. This scenario was assumed to be the most controlled and experimentally repeatable. In each of the studied replicates (see appendices 1, 2 and 4 for more information), pressure readings were recorded at velocity intervals of 0.05 m/s.

The open channel (Figure 2.2.b) comprises a free surface rectangular canal with an adaptable slope that can reach different regimens through the modification of the discharge and the slope. In normal operation ranges, a velocity range from 0.1 m/s to 1.5 m/s can be obtained. A complete description of the experimental setup can be found in appendices 3 and 4. The measurements were conducted from 0.1 m/s to 1.4 m/s in steps of 0.1 m/s.

The vertical slot fishway (VSF) (Figure 2.2.c) offers the most challenging conditions. Fishways are artificial structures designed to allow the passage of fish through transversal obstacles to the river (e.g., dams, weirs, and others). VSFs are characterized by a wide spectrum and contrast of turbulence intensities, such as environments expected in the field, and they present a possible target scenario for the use of ALLs as environmental monitoring devices. A complete description of this structure and the complete experimental plan and data treatment can be found in appendices 1 and 6, and in [97]. For this setup, two different discharges were measured (0.130 m³/s and 0.170 m³/s) at three different depths (20%, 40% and 60% of the mean water level) according to the point distribution depicted in Figure 2.2.c. The measured velocities ranged from 0.1 to 1.4 m/s.

In addition to these scenarios, in appendix 2 a supplementary validation test was conducted. This consisted in four locations with different turbulence levels of *Keila river* (Estonia) (Figure 2.3). The measured velocities ranged from 0.61 to 1.2 m/s.



Figure 2.3. Different locations measured in Keila River, Estonia. The turbulence level increases from a to d.

2.3. Hydrodynamic variable estimation approaches

The main objective followed in this first step of ALL research was *to make hydrodynamic variable estimation with absolute pressure sensor-based ALLs in real-world conditions possible*. Previous studies on absolute pressure sensor-based ALLs used Bernoulli's principle to calculate the flow velocity [13], [24], [26], [27], [65]. Therefore, the first classical approaches were tested using the closed flume setup. However, limitations that would make this approach difficult to use under real-world conditions were detected. Thus, alternative approaches were designed to extend the applicability of absolute pressure sensor-based ALLs: mixed approach, statistical approaches and neural network approach.

2.3.1. Classical approach and its limitations

The interaction of the flow over a rigid body will generate different pressure distributions around the body, according to the body's shape and orientation, its surface properties, the flow velocity, and fluid properties. Considering this effect and the presence of a constant component of the pressure related to the depth (assuming quasi-hydrostatic conditions), the pressure difference between two given points on the body surface will be the same for each flow velocity (assuming inviscid, incompressible, irrotational and steady flows) (*Figure 2.4.a*). Considering this physical effect, which is also described by Eq. (2), a relation between pressure and velocity is established (*Figure 2.4.b*).

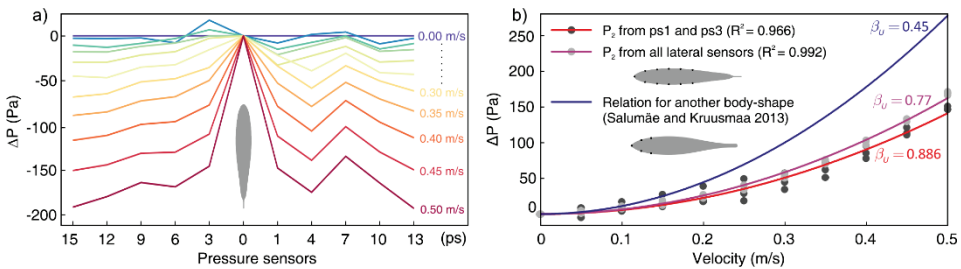


Figure 2.4. Results of the application of the classical approach using the ALL under study [50]. a) Mean pressure relative to the nose sensor (ps0, Figure 2.1) during the first replication of the close flume experiment. b) Mean pressure differences for the two combinations of pressure sensors and another body shape versus flow velocity.

For the studied prototype (and in general National Advisory Committee for Aeronautics (NACA) shapes), the front part will sense the maximum pressure (stagnation pressure), and progressively, the pressure will be reduced when the sides are approached (Appendix 1). Considering this and through the application of Bernoulli's principle, the accurate estimation of velocity appears to be possible. However, during the application of the studied prototype using the classical approach, some limitations were identified for the use of absolute pressure sensor-based ALLs:

1. **Depth-sensitivity relation.** The sensor sensitivity is inversely proportional to the maximum measurable pressure. Therefore, considering that small sensitivities are required to sense small velocities (*Figure 2.4.b*), the minimum estimable velocity will be defined by the maximum measurable pressure by the pressure sensors.
2. **Hydrostatic pressure differences.** Considering the pressure caused due to the water column (hydrostatic pressure, $P = g \cdot h \cdot \rho$, where g stands for gravity, h for

water column, and ρ for the density), small water level column differences between sensors have the potential to generate small pressure deviations.

3. **Turbulence.** In many natural conditions, the movement of fluids does not form a streamlined, orderly flow. Therefore, an instantaneous measurement will be far from the pressure distribution profiles represented in *Figure 2.4.a*. These profiles will be achieved by averaging a certain number of measurements that will depend on the freestream flow properties (velocity and turbulence) and the sampling frequency as well as the sensitivity of the measuring device.
4. **Temperature.** Pressure sensors and analog to digital converters, like any other measurement devices, are subject to errors caused by changes in temperature. These variations may be controlled if the temperature of individual sensors is monitored. However, the heating caused due to electronic hardware, the cooling effect caused due to the flow influence, together with the environmental temperature will provoke non-linear processes over the ALL body. These processes will be difficult to model without precisely controlling the environment and will be more important for sensors with large measuring ranges. The density of the fluid is also temperature dependent and thus, assuming a constant density neglects changes caused by the water temperature.
5. **Noise-pressure range relation.** In general, the absolute level of the expected noise (e.g., electronics, temperature, etc.) will be higher for sensors designed for measuring higher pressures. Therefore, the expected errors in hydrodynamic variable estimations due to the noise will be higher for pressure sensors with higher pressure ranges.

Similar limitations have also been reported in other specialized publications, e.g., [9], [27], [34], and they provoke the need of calibration prior to their use and from test to test. For instance, [34] reported a calibration procedure every 3 minutes. In all the cases reported, the calibration procedure consisted in still water measurements to determine offsets between sensors. This calibration plan is possible to apply under controllable environments where still conditions can be induced; however, it is difficult under real-world applications. Therefore, alternatives to the physical approach are necessary for hydrodynamic variable estimation under real-world applications. In the following sections, we summarize the three approaches tested to solve some of the detected limitations (mixed approach, statistical approaches and neural network approach).

2.3.2. Mixed approach

The first approach tested to solve some of the detected problems was the mixed approach [50] (Appendix 1). This approach entails the application of a two-step procedure: a statistical approach to estimate the mean value of the target variable and a physical approach to recover the value of the variable in relation to the original sampling rate (*Figure 2.5*).

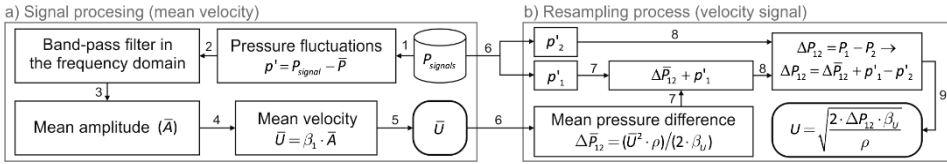


Figure 2.5. Signal processing and resampling process flowchart [50]. a) Mean velocity calculation. b) Resampling process.

Considering that the time-averaged value of the pressure is altered by the limitations defined in the previous section, it will be necessary to determine a feature that can override those limitations. One of these features is the pressure fluctuation (p').

It was observed that the increase in velocity and turbulence tends to produce higher pressure signal fluctuations and for the considered data was leading to an average increase in the pressure signal's amplitude. Similarly, in contrast to absolute pressure, their rapid nature makes them resistant to most of the problems listed in the previous sections.

Considering this principle, it is possible to employ this feature as an estimator of hydrodynamic variables. The amplitude of fluctuations can be obtained by translating it into the frequency domain through the fast Fourier transform (FFT) and the subsequent application of a band-pass filter (BPF) to separate the target hydrodynamic variable from other possible influences. In the case of velocity, the relation with the signal amplitude can be modeled by a linear regression (Figure 2.6).

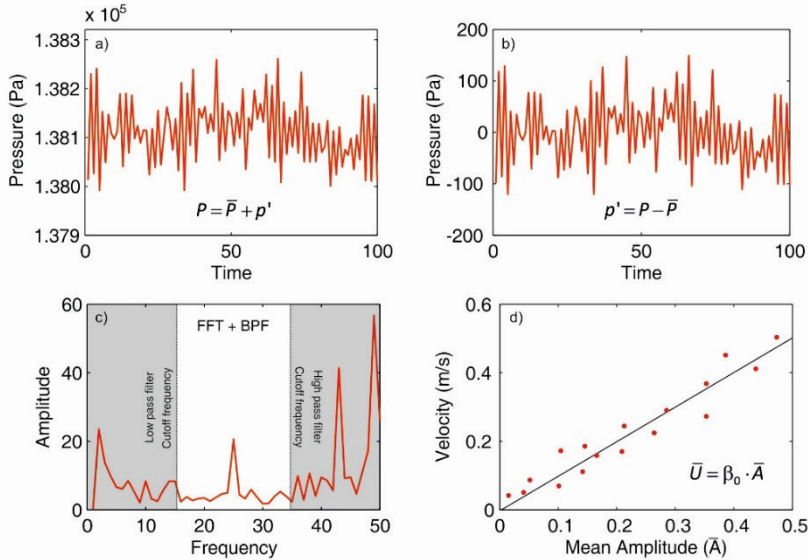


Figure 2.6. Graphical representation of the signal processing pipeline. a) Raw pressure data; b) Fluctuation extraction. c) Translation to frequency domain [fast Fourier transform (FFT)] and filtering [band-pass filter (BPF)]. d) Representation of the mean amplitude and velocity fit.

To apply the method, two parameters must be determined: the total signal duration and the filter cutoff frequencies. Both parameters should be determined using the velocity data obtained from different experimental conditions.

The algorithm will deliver a mean velocity estimation over a long sampling time. Consequently, to estimate the dynamic properties of the flow (such as turbulence intensity), it will be necessary to resample this velocity into the original sampling rate. This can be achieved by taking advantage of the physical approach as illustrated in *Figure 2.7*.

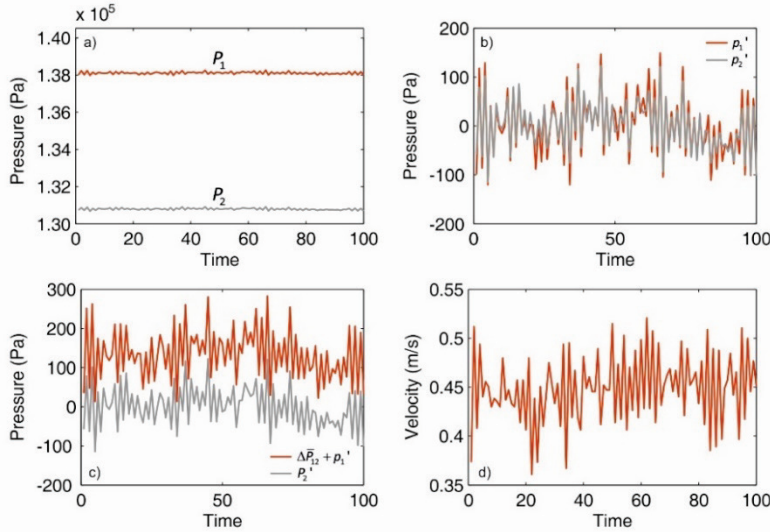


Figure 2.7. Example of the resampling process. a) Raw pressure signal at two different pressure port locations, P_1 and P_2 . b) Subtracting the time-average to obtain the zero mean fluctuations. c) Calculation of $\Delta \bar{P}_{12}$ considering \bar{U} (with Pitot relation) and adding it to p_1' . ΔP_{12} signal will be equal to $\Delta \bar{P}_{12} + p_1' - p_2'$. d) Velocity signal calculation with Pitot equation after ΔP_{12} signal calculation.

In [50] (Appendix 1), this approach was tested using the close flume and the fishway experimental setups. The validation consisted in testing its performance using independent fishway datasets. *Figure 2.8* shows as example the contour plots estimated with the artificial lateral line in comparison with the obtained with a laboratory ADV.

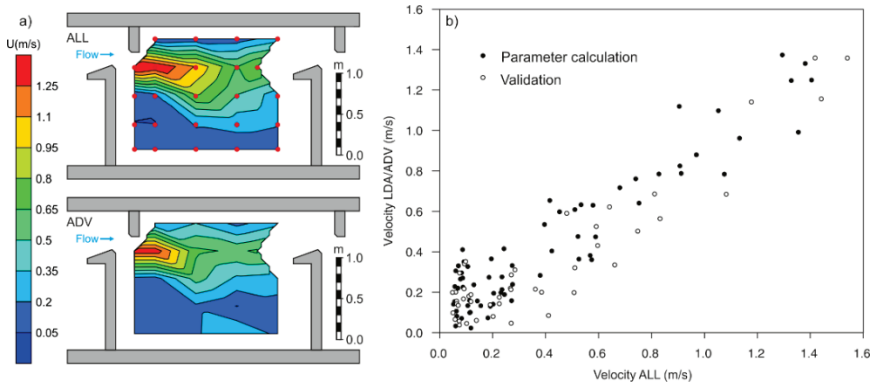


Figure 2.8. Validation of the approach [50]. a) Comparison between the profiles estimated by the ADV and ALL in $0.17 \text{ m}^3/\text{s}$. b) Scatter plot of the measured velocities for approach parameter calculation (ALL vs DVL) and for validation (ALL vs ADV, $R^2=0.837$).

2.3.3. Statistical approaches

The applicability of the statistical approaches can be further extended by using them to estimate both velocity and turbulence metrics, leaving aside the classical approach. *Figure 2.9* summarizes the proposed workflows for the hydrodynamic variable calculation. A detailed algorithmic description for the calculation of velocity can be found in [49], [51] (Appendices 2 and 6) and for turbulence metrics in [49] (Appendix 6).

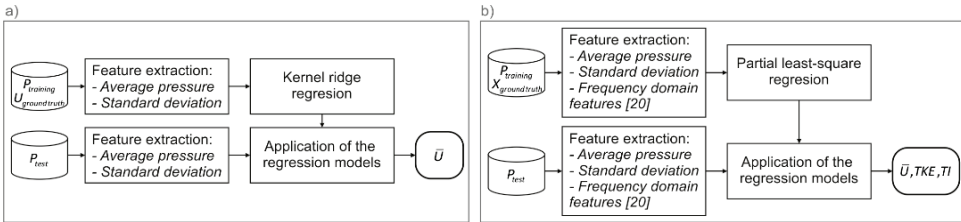


Figure 2.9. Statistical workflows for hydrodynamic variable's calculation. a) Preliminary workflow for velocity estimation [49]. b) Extended workflow, X represents other possible features [51].

Both statistical methods (*Figure 2.9*) utilize the standard deviation of the signal as main feature. Standard deviation of the signal shows a strong correlation with pressure fluctuations defined before. Similarly, the second method (*Figure 2.9.b*), also utilizes the average pressure and frequency domain features (defined as X in *Figure 2.9.b*) which seems to increase the predictability of the method, even if the contribution of these variables is rather small.

The validation of the approaches, in both cases, were performed by means of independent tests (Appendix 2 and 6), comparing the estimated result with observed ones. First approach (*Figure 2.9.a*), provided errors lower than 0.1 m/s for velocity estimates and, moreover, it demonstrated the ability to correctly estimate the velocities in a natural river (Keila river (Estonia)) (*Figure 2.3*). The second approach increased the performance of the previous one by offering a mean absolute error for all the estimated variables between 8.5 % and 15.3 %.

In addition, both approaches are compatible with the resampling process defined for velocity in the mixed approach. That is to say, after the calculation of the mean velocity, the workflow defined in *Figure 2.7* could be applied.

2.3.4. Neural network approach

Previous methods suffer from higher errors when estimating low velocities (Section 1.5). This is due to the requirement of high sensor sensitivities to estimate low velocities, as well as, the pressure distortion levels of the studied environments. Therefore, large sampling intervals are required to improve the accuracy of the estimates.

However, the exploitation of the distributed and synchronous sensing capacities of the studied prototype seems to improve the estimations in the lower ranges. To achieve this, in appendix 4 the product-moment correlation coefficient between sensor pairs are proposed as features. After these feature are used to train an artificial neural network (ANN) for current velocity estimation (*Figure 2.10*).

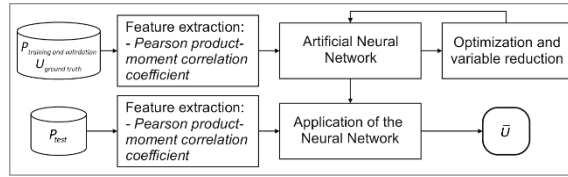


Figure 2.10. Proposed neural network approach for current velocity estimation.

The combination of all the pairs of sensors used [11, the ones situated in the middle plane of the sensor body (*Figure 2.1*)] yields a 55-dimension feature vector as an independent variable. First, the structure of the ANN is analyzed to optimize the number of layers, transfer function, and the number of neurons (Appendix 4). This is achieved through comparisons of the performance of different neuron combinations and the evaluation of their improvement using Student’s t-test and random trials (60% training, 20% validation, and 20% test, for all cases). For variable reduction, after the ANN structure is defined, a stepwise method adapted to ANN was designed. This method progressively reduces variables with regard to the significance of the model post their elimination. Using this method, the feature vector is reduced from 55 to 11 cross-correlations (*Figure 2.11*), without a significant loss of the model’s predictive power. A similar approach is used also to estimate the relevance of each of the final sensor pairs used.

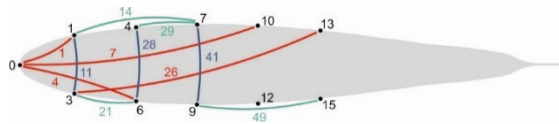


Figure 2.11. Final 11 correlations used in the model. The classification in terms of significance can be found in [1].

The approach was applied to close flume, open channel flume and fishway data, showing a high correlation with the measured data ($R^2 = 0.911$, using 11 correlations coefficients) and a mean absolute error of 0.066 m/s.

2.4. Method Comparison

Mixed and statistical approaches share some commonalities: (1) mean pressure fluctuations are correlated with the standard deviations of the velocity signals and (2) the sensor signals, contrary to the neural network approach, are treated individually. Therefore, similar performances are expected.

Figure 2.12 depicts results from the open channel experimental setup for mixed and statistical (kernel ridge regression) approaches (a) (Appendix 3) as well as for all the studied scenarios with regard to the neural network approach (b) (Appendix 4).

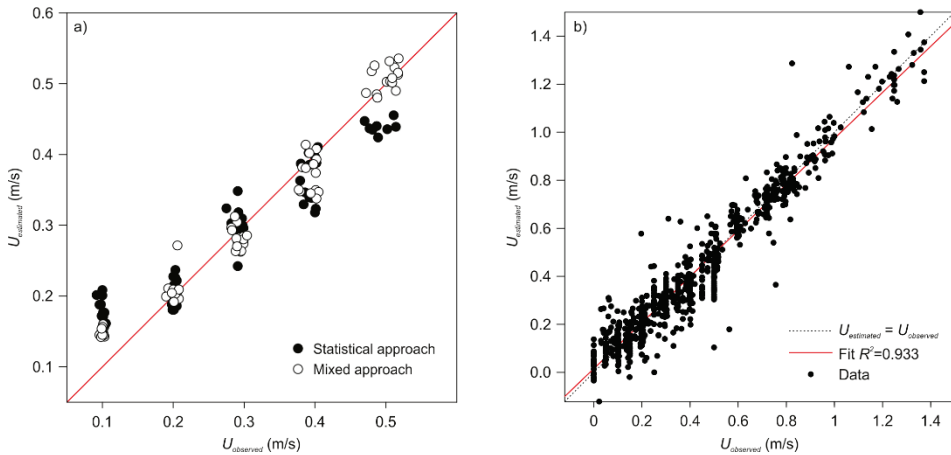


Figure 2.12. Velocity fit plots for the different estimation approaches. a) Mixed ($R^2 = 0.959$) and statistical (Kernel ridge regression) ($R^2 = 0.920$) approaches in the open channel experimental setup [68]. b) The neural network approach using all experimental setups [1].

The mixed and statistical approaches tested had a tendency to overestimate low velocities. This can be explained by the sensitivity and the range of the sensors used (sensitivity is inversely proportional to the range), the quadratic relation between flow velocity and pressure (lower velocities will require higher sensitivities) or because they assume a single model. In this sense, longer measuring times will be required for low velocities as pressure signals will be closer to the sensitivity of the sensor. However, the combination of sensor pairs together with the neural network learning algorithm appears to overcome this limitation to some extent, as can be observed from the results of the neural network approach.

The dependency on the number of samples for the average velocity's estimation will also make the error time dependent. Figure 2.13 shows the evolution of error for the mixed approach [50] and the neural network approach [1] as well as the optimal solution for the statistical approach (partial least-square regression [49]). From the figure, it can be noted that the overall performance of the approaches is very similar. The need of large signal durations is one of the major drawbacks of all the approaches proposed. In the same way, the data can be highly non-stationary, and thus, it is very unlikely that performance will significantly improve with progressively longer sampling durations.

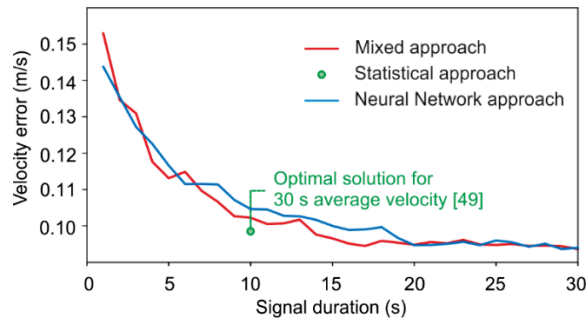


Figure 2.13. Error evolution with the proposed methods. It should be noted that in the original article of the statistical approach a 10 s signal was used to calculate a 30 s average velocity, thus the model performance of this reference was non-ideal.

Regarding turbulence, the statistical approach described in appendix 6 (Figure.2.5.b) directly estimates the possible variables of interest (e.g., turbulence kinetic energy, Reynold stresses, turbulence intensity, among others). The original article is referred to examine the different performances (Table 8 and 9 in Appendix 6). The mixed approach offers certain limitations regarding turbulence. It only allows the recovery of the original velocity fluctuations and thus only the turbulence intensity can be calculated. Figure 2.14 presents the comparison of velocity distribution of an ADV against the ALL for the test conducted in the open channel flume. The observed distribution seems in the same range, increasing towards the higher velocities; however, it should be noted that the sampling rate of both the technologies is different (for this case, the ADV was a Sontek Flowtracker with a sampling rate of 1 Hz, whereas the ALL sampling rate was 250 Hz).

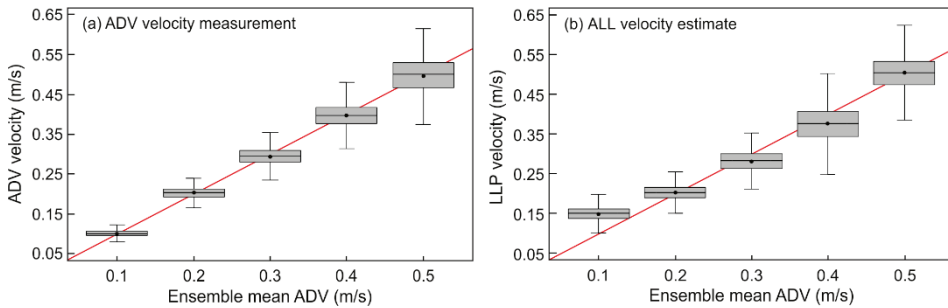


Figure 2.14. Comparison of the (a) ADV measurements and (b) ALL velocity estimates using the mixed approach. The sample sizes for the ADV measurements (0.1, 0.2, 0.3, 0.4, 0.5) m/s were (2100, 2100, 2160, 1560, 1320) and 56251 for each ALL velocity estimate [68].

Considering the limitations of each method, if we are interested in measuring all the common turbulence variables, it will be necessary to employ the statistical approach. Regardless, if the velocity distribution over time is to be examined, for a frequency analysis or a specific analysis of short time events, or simply to calculate the turbulence intensity, the mixed approach serves the purpose (Figure 2.15). The estimation of turbulence metrics considering the neural network approach still needs to be explored.

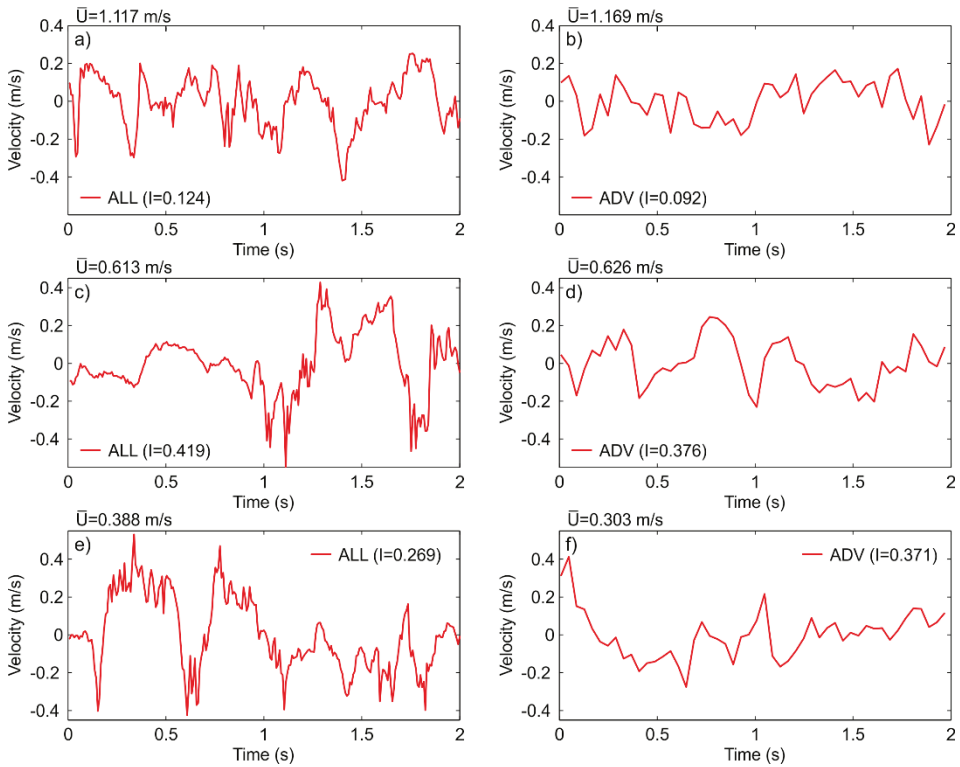


Figure 2.15. Velocity fluctuations (u') measured with ADV (25 Hz) and LLP (125 Hz) for the third experimental configuration (vertical slot fishway with a discharge of $0.130 \text{ m}^3/\text{s}$ at water level of $0.6\text{-}h$). The signals have the same duration and location, but they were not measured simultaneously. a) and b) Slot. c) and d) Jet region. e) and f) Recirculation region.

2.5. Map based localization using hydrodynamic variables

The proposed approaches have direct application in the characterization of underwater environments as they allow the estimation of the hydrodynamic properties of the fluid media. Later, by exploiting these properties, we can solve more complex real-world applications. To show this, in [39] a conceptual method to solve underwater localization problems using hydrodynamic variables sensed with an ALL and simulated hydrodynamic maps as *a priori* information is proposed (Appendix 7).

Localization is one of the basic problems of any autonomous robot [98], as the robot needs to know its location to perform more complex tasks. Underwater localization can be achieved in many ways: dead-reckoning [99], through the use of *a priori* available maps (map-based localization) [100], or through simultaneous mapping *a priori* unknown environment and keeping track of one's location on it (i.e., SLAM) [101].

Map-based localization is an interesting alternative when maps for the environment to be explored are available; for anthropogenic environments such as harbors, sewers, or other types of drowned structures, or natural environments such as caves [102].

The most common sensing modalities used to perform underwater localization are vision and sonar. Both sensing modalities might be of limited utility in some environments, such as homogeneous or turbid ones. Therefore, the combination of

different sensing modalities can constitute the most interesting alternative to perform successful localizations. In this regard, flow sensing can provide an interesting alternative or complement to achieve effective localization. For instance, in [13] and [22], 1D localizations were performed using the velocity change generated through the interaction of flow with a specific obstacle.

The method here proposed is a generalization of the one proposed in [35], which uses the studied prototype (Section 1.3) and the third scenario for localization (fishway, Figure 2.2.c). In the method proposed in [35], two main problems were detected: (1) the features used from the prototype had an abstract nature, making it impossible to use in other environments without a pre-calibration of features and (2) the method required, previous to the localization and for each possible hydrodynamic scenario, a *a priori* scan to construct the map of the features for localization. Here these limitations are solved by replacing the abstract feature with velocity estimates using mixed approach (Section 1.4.2.) and by using simulated maps as *a priori* information of the environment (Figure 2.16).

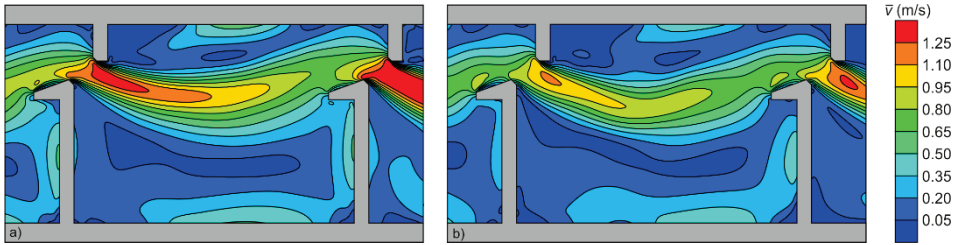


Figure 2.16. Simulated maps used for the two studied discharges, at 40% water-column height [39]. Both have been calculated using RANS technique (*k*-epsilon model, grid size = 0.05 m). a) Discharge rate of 0.17 m³/s. b) Discharge rate of 0.13 m³/s.

The localization problem is solved offline using particle-filtering (see a complete description in [35], [39]) (Figure 2.17). In the beginning ($t = 0$), a set of m particles X_t are randomly scattered through the available simulated map (Figure 2.16). Each particle i has an associated weight ($w_{t,i}$), which is the probability of being the current position of the robot. Until the first observation (U_t , sensed flow velocity), weights are equally distributed. After a motion step (d_t) and an observation, weights are updated, and particles resampled accordingly (i.e., the probability of a particle being sampled will be proportional to its weight). Therefore, at any given time, the mean value of the resampled particles will represent the estimated position of the robot. The update in weights is made in relation to comparisons with the value of velocity according to particle position in the simulated map with the observation of the robot.

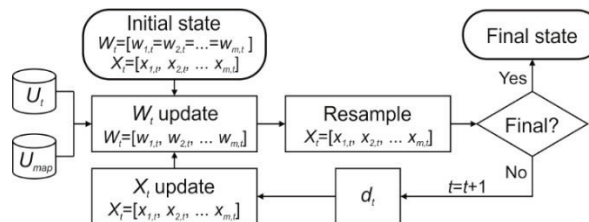


Figure 2.17. Particle-filter algorithm used in this study. U_t represents the set of estimated speeds until t , and U_{map} the set of velocities in the simulated map [39].

Figure 2.18 shows an example of the algorithm’s performance; the real position of the robot is represented in green, while the trajectory based on control inputs is depicted in blue. In the first state, the particles are distributed randomly throughout the maps (Figure 2.18.a). After, with each new measurement and motion, the position is updated (Figure 2.18.b-c). Figure 2.18.d depicts the evolution of the absolute localization error over different states.

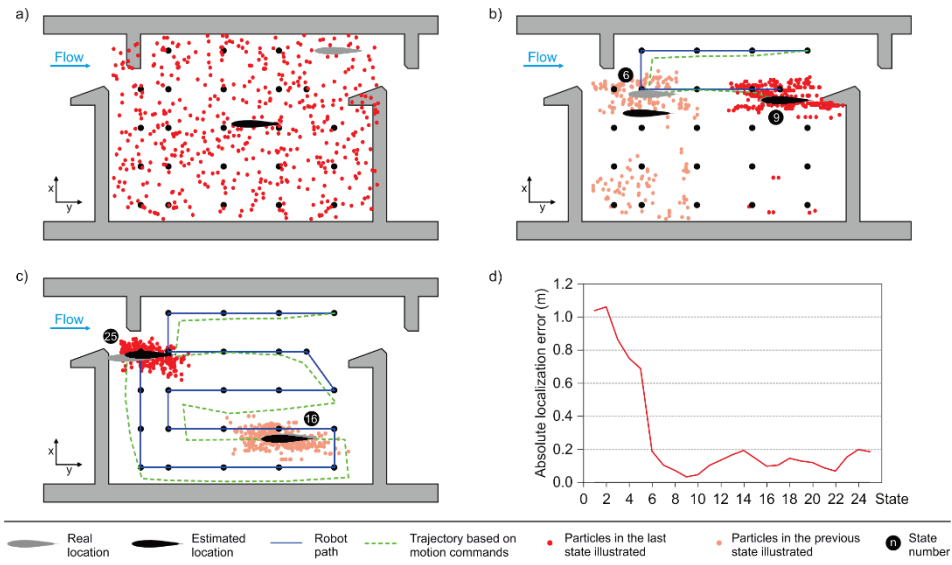


Figure 2.18. Simulated map-based localization in 2D; $\sigma = 0.20$, 500 particles, $0.40h_0$, and $0.17 \text{ m}^3/\text{s}$ [39]. a) Initial state. b) 6th and 9th states. c) 16th and 25th states. d) Evolution of the localization error.

The algorithm performance is validated using different hydrodynamic scenarios in the fishway, introducing normally distributed random errors in the motion steps and measurements as well as different particle densities (Appendix 7).

The values appear to be independent of the number of particles used, and the error increases, logically, whenever the artificially introduced motion and measurement errors increase (Table 1, Appendix 7). All studied cases demonstrate convergence at the real location of the prototype, and this is accelerated when the flow field’s heterogeneity increases. Therefore, the results not only indicate the possible use of flow sensing for localization in hydrodynamically diverse structured environments but also demonstrate the potential of flow sensing for incorporation into underwater navigation in conjunction with other sensing modalities such as sonar, vision, or DVLs.

However, it is worth mentioning that the flow velocity estimation approach used (as well as, the rest of the proposed approaches) required a certain amount of time to provide accurate velocity estimates. This highlights one of the biggest problems that is necessary to overcome in order to apply ALLs in underwater robotics: real-time availability of estimates.

2.6. Summary and conclusions

In this chapter, an absolute pressure sensor-based ALL that gathers the latest advances in pressure sensor-based ALLs is studied for hydrodynamic variable estimation. The analysis of classical relations to estimate flow velocity using pressure showed limitations for their use under real-world conditions. Therefore, to overcome these limitations new hydrodynamic variable estimation approaches were defined. The proposed approaches demonstrate accurate performance for the time-average velocity estimation as well as turbulence metrics. Concluding that by selecting correct features it is possible to find alternatives for hydrodynamic variable estimation when pressure sensor calibration procedures before each test are impossible and under a wide spectrum of hydrodynamic conditions.

However, all the approaches defined need long signals (10 to 30 s) to estimate average hydrodynamic variables or their time series. The need of long signal for variable estimation limits the use of these approaches in applications such as the localization method proposed in Section 1.6. Additionally, these approaches have a significant empirical component and to apply them to other body shapes or sensor combinations, they will be required to run again for different test cases.

Depth-dependency relation seems one of the major drawbacks of absolute pressure sensor-based ALLs. The contribution of the water column pressure in the sensor is usually more important than the velocity contribution that drives to low sensitivities when high depths are expected. This will limit the measurement of low velocities and increase the recording times to estimate them. In addition, the possible distortions from other factors, such as temperature, will be higher in sensors designed for higher pressure ranges.

Considering the limitations encountered, the following chapter is focused on the design of a new ALL generation capable of surpassing the problems and limitations of previous designs through: (1) the increment of sensitivity using differential pressure sensors, (2) the reduction in the temperature exchange through the selection of a specific sensor, (3) the development of a differential pressure-velocity relation able to provide real-time velocity estimates, and (4) the selection of well-known body shapes that will allow an easier extrapolation of the findings and relations to other ALLs.

3. Development of differential pressure sensor-based ALLs

In the previous chapter, it was concluded that absolute pressure sensor-based ALLs suffer from some drawbacks that could limit their usability in some applications and environments. For instance, in contrast to differential pressure sensors, absolute pressure sensors also measure pressure due to the water column height; therefore, applications in high depths may suffer from a sensitivity limitation. In the same way, it was found that, with the proposed approaches, real time estimation of variables was a difficult task (only available in some idealized conditions).

This chapter shows how these limitations are partially overcome by designing a new ALL based on differential pressure sensors. For this, a novel approach that uses high sensitivity air differential pressure sensors was developed and tested. Moreover, a general relation between differential pressure sensor-based ALLs output and velocity was developed. This relation can provide accurate instantaneous estimates of velocity independently of the angle of attack of the body where the lateral line is applied.

During the alternative analysis and design, basic engineering principles were considered to provide a solution that is easily adaptable to different target applications. This is demonstrated by applying the differential pressure sensor-based ALL to several prototypes (Appendix 5 and 8).

3.1. Prototype development

The development of the lateral line was distributed into two main steps: (1) shape selection and (2) sensor selection.

3.1.1. Shape

A common feature across most absolute pressure sensor-based ALLs listed in the introduction section is the absence of rules for shape selection. This makes it difficult for them to adapt to other possible devices and makes running new tests to model their performance necessary.

For instance, the shape of the ALL used in the previous chapter (Chapter 2) was obtained from a 3D scan of a farm-raised rainbow trout (*Onchorynchus mykiss*). At first glance, this can be perceived as a good idea, as one of the motivations of the device was to evaluate the preferences of fish fauna. However, its biomechanics are completely different from that of a real fish [103]. Therefore, despite sharing a similar appearance, the interactions of the ALL with the fluid media remain different. Regardless of this, the main properties of interest were still preserved: (1) distributed sensing, (2) measurement of fluid-body interactions, and (3) high sampling frequency.

In view of this, similar goals could be achieved using shapes that achieve a bigger grade of standardization. The use of well-known shapes would allow the translation of collected knowledge into new prototypes more easily. In this regard, two main target shapes were considered for the new design: NACA and circular shapes. Finally, the circular shape was considered for the preliminary tests because (1) they are one of the most studied shapes in fluid mechanics (*Figure 3.1*), (2) their geometrical characteristics provide an easier way to develop them, and (3) this shape is used in many target underwater applications (e.g. underwater robotics).

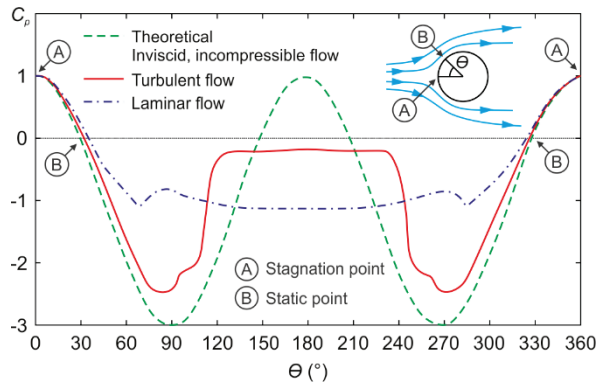


Figure 3.1. Pressure coefficient ($C_p = 1 - (v/v_{max})^2$) distribution over a circular cylinder under laminar and turbulent air flows according to the angle (θ) from stagnation point (modified from [104]) [82].

The fluid motion over circular shapes has been widely studied [104] as well as previously used for flow velocity estimation in aeronautics [75], [79] and in Fehcheimer probes [105]. This provides a theoretical framework to develop our prototype and models. For instance, with the knowledge about the expected pressure distribution over the circular shape (Figure 3.1), we can select *a priori* the optimal positioning of the pressure sensors and know the effects of alternative positionings.

3.1.2. Sensors and electronics

As previously discussed, differential pressure sensors were selected due to the multiple advantages offered in contrast with absolute pressure sensors. However, one of the limitations of measuring pressure in water is the stiffness of the membranes used to ensure sensors' water tightness. This stiffness creates difficulties for measurements in low-pressure ranges; thus, sensors with the following required characteristics are not commercially available: (1) differential, (2) small dimension, (3) small pressure range (± 2000 Pa), (4) temperature compensated, and (5) water resistance.

That being the case, to overcome these limitations, air pressure sensors capable of supporting high humidity concentrations, including a rigid vertical tubing system to ensure correct phase separation (i.e., water air separation), were proposed.

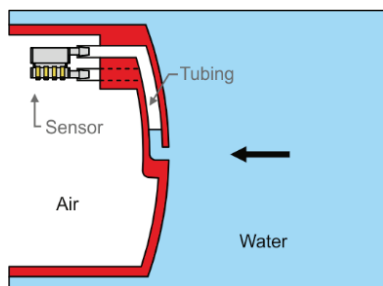


Figure 3.2. Sketch of the solution used for phase separation.

The tube for phase separation opens the opportunity to use a wide range of differential pressure sensors. Table 3.1 shows electronic configurations tested and recommended for applications that aim to measure velocities up to 1.5–2 m/s. For these electronic combinations, no significant difference was observed [82]. In view of this,

analog sensors were selected as the final optimal alternative for our future prototypes as (1) they allow control of the amplification and sampling rate more easily, (2) the black-box effect of digital sensors is eliminated, (4) they are cheaper, and (3) their pressure range is optimal.

Table 3.1. Different electronics configurations recommended to develop prototypes [82].

Component	Analog	Digital
Microcontroller board		Arduino Micro
Pressure sensors	MPXV7002	SSCDRRN005ND2A5
Range	± 2000 Pa	± 1244 Pa
Maximum pressure ($P_A > P_B$)	75000 Pa	4903.325 Pa
Temperature sensor	ADT7301 (13 bits)	On-board
Multiplexer	-	TCA9548A
Analog to digital converter	16 bits–LTC1867	14 bits–on-board
Resolution	0.0695 Pa	0.03 Pa
Tested sampling frequency	200 Hz	100 Hz
Maximum sampling frequency	> 400 Hz	200 Hz

3.1.3. First physical prototype

Considering the above information, a first prototype was developed to probe the concept and to test the applicability of the proposed design and methods (Figure 3.3). This prototype consisted of a 3D-printed “bullet-shape” cover with an underwater box wherein the electronics as well as sensor ports were allocated. In this prototype, the sensor ports were connected to the front part of the bullet shape cover through silicon tubing. This design was conceptualized as modular to study the different pressure sensors and pressure port separations.

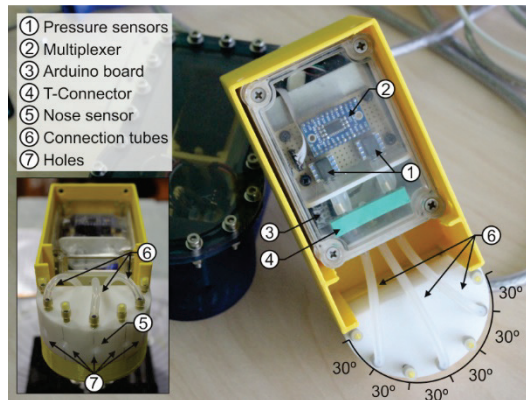


Figure 3.3. The prototype used in the experiments (B-Box). The top cover has been removed to display the internal components.

The electronics tested in this design correspond to the digital alternative defined in Table 3.1. They were selected as the first testing alternative due to their higher sensitivity. Two sensors were used for this design. Each sensor’s first port was connected

to the nose plug through a T-connector (4, *Figure 3.3*). The second ports were tested under different angles in side ports, with one sensor on each side.

A more detailed description of this first prototype can be found in [62] (Appendix 5).

3.2. Performance evaluation

The prototype was evaluated using the first scenario defined in Section 2.2 over a range of velocities from 0 to 0.5 m/s and 4 different angles of attack (0°, 15°, 30°, and 40°). *Figure 3.4.a–b* summarized the results of the first test. When the prototype faced the flow, the signal of both sensors (ΔP_1 and ΔP_2) was found to be equal; however, they changed accordingly when the angle of attack was modified. Considering the distribution of pressure in relation to the velocity during different angle configurations, the distribution can be defined by the conic function Eq. (3).

$$U = \sqrt[4]{a(\Delta P_1^2 + \Delta P_2^2)} \quad (3)$$

where a is a coefficient that depends on the pressure sensor plug distribution. Ideally, when the second sensor plugs are subject to the freestream velocity (for cylinders 30°, $C_p = 0$, *Figure 3.1*), a will be equal to $(2/\rho)^2$. Similarly, the pitot equation is apparent in the relation (for an angle of attack of 0°, $\Delta P_1 = \Delta P_2$, then Eq. (3) becomes Eq. (2)).

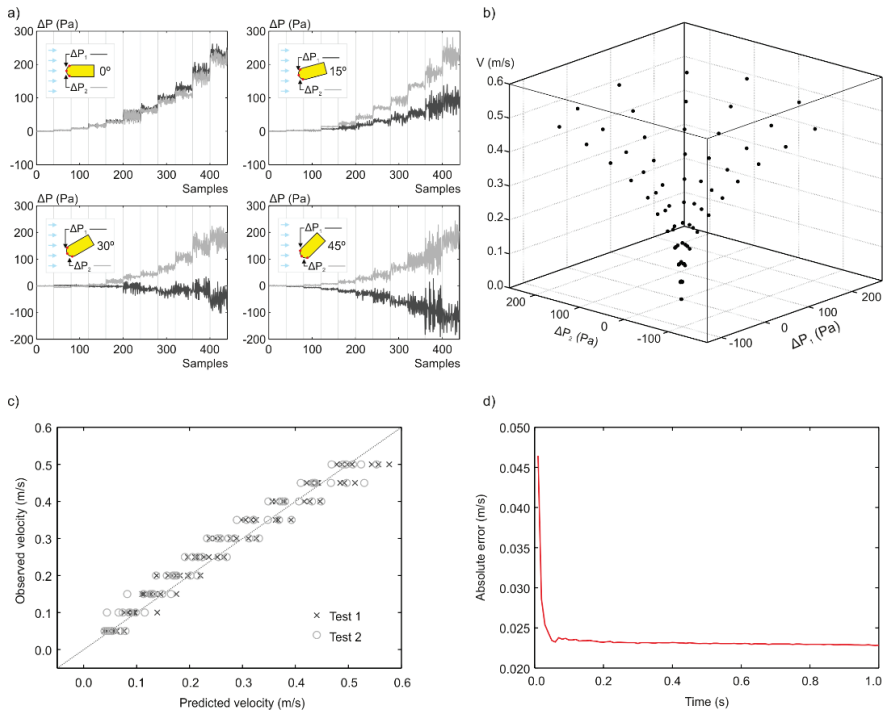


Figure 3.4. Summary of the experimental results [62]. a) Example of pressure distribution for each velocity (different steps of each graph) and for different angles of attack (only 1 second of the signal is shown). b) The result of all studied scenarios in the first run of experiments (second plugs connected at $\pm 60^\circ$, in Eq. (3) $a = 1.32 \cdot 10^{-6}$, $R^2 = 0.9641$); c) Observed velocity against predicted velocity for all tests. d) Evolution of the mean absolute error as a function of increasing signal sampling duration.

In Figure 3.4.c, the relationship between the estimated and observed velocity is presented, where test 1 was used to calibrate the model while test 2 was considered a replicate to validate the model (each velocity is subject to 4 angles of attack). Contrary to the observations from some of the approaches defined for the absolute pressure sensor (Figure 2.11), the low velocities have been correctly estimated. One of the reasons of the improvement of low velocities estimation is the increment of the system's sensitivity. In the same way, it is possible to maintain at any depth this sensitivity due to the differential pressure.

Similarly, due to the sensitivity and reduction of the noise sources, a smaller number of samples are required to reach a stable mean value of the velocity (Figure 3.4.d). The effective sampling rate for the mean velocity is > 10 Hz, a value that is far from that obtained in previously studied approaches (Figure 2.12) and opens the door for online applications of this technology.

Additionally, only two pressure sensors and two variables were used to estimate the velocity and its fluctuations over time. With this reduction of hardware, the resources required to perform the same task, i.e., energy and computation power, are reduced. Similarly, the defined model gains a physical basis, and it will be possible to apply it to other prototypes. This has been confirmed in the multiple prototypes designed after the first one (Chapter 4).

Regarding the design, it is worth mentioning that the deployment of the system due to the interphase separation (air-water separation) will generate an offset that should be considered to obtain more accurate velocity estimations. For application in environmental monitoring, this offset has been dismissed, which has resulted in good results (Section 4.2), and for underwater vehicle applications (Section 4.1), the initialization protocols can be developed to calculate the offset before a mission.

3.3. Developed ALLs prototypes

After the first conceptual design, multiple prototypes were developed for their use in field applications. All the developed devices have been deployed successfully in field and have produced valuable data for different applications (e.g. turbulence estimation, fish habitat studies or underwater velocity estimation).

3.3.1. D-Box

D-Box is a compact field-ready flow measuring device that is not only able to sense the pressure differences on its body but also record them simultaneously. Its main field of application has been the turbulence calculation in hydropower intakes [83], [106]. In order to achieve this, the prototype is equipped with 2 differential pressure sensors (0-4000 Pa MPXV5004) and one gauge pressure sensor (0 to 10000 Pa MPX5100GP) connected to an Arduino Uno with a datalogging shield (real time clock and SD card) and a battery that powers the device (Figure 3.5).

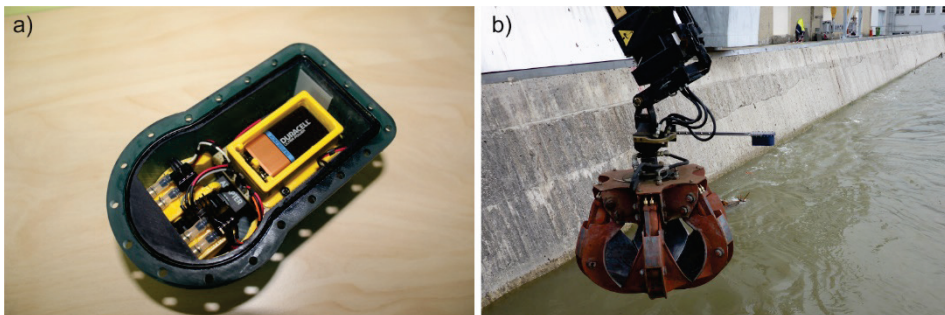


Figure 3.5. a) Electrical components of D-Box. b) Field deployment of D-Box.

3.3.2. iRon

iRon is an ALL probe developed for environmental monitoring. The aim behind this idea is that ALL mimics, up to some extent, the sensory system used by fish; therefore, it could be a way to measure the flow characteristics from the fish's perspective. iRon was scaled to the size of a barbel, a 0.22 m long NACA025 streamlined body. It can measure a stream-wise pressure gradient simultaneously using six differential pressure sensors (± 2000 Pa MPXV7002) that are amplified by a 16-bits A/D converter (LTC1867). Additionally, the water depth is measured by the probe using a gauge pressure sensor (0 to 10000 Pa – MPX5010GP) (Figure 3.6). The device can measure up to 400 Hz.

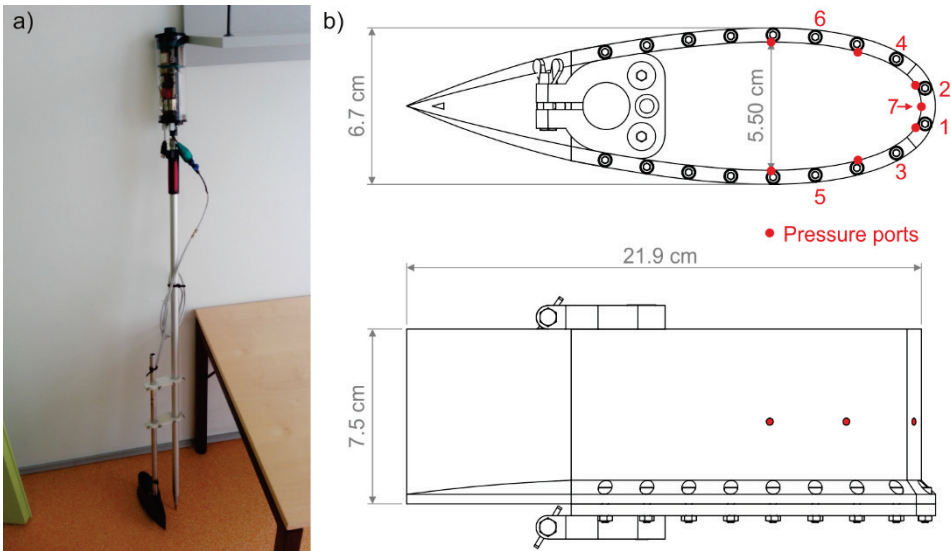


Figure 3.6. Lateral line probe (LLP) used to measure body-oriented pressure gradients. The NACA025 body shape is outfitted with six differential pressure sensors (1 – 6) and one absolute (7) pressure sensor. a) Probe ready for its field use. b) Sketch of iRon.

3.3.3. DPSS

The first generation of “Differential Pressure Sensor Speedometers” (DPSS) was designed to be used in torpedo-shaped AUVs with interchangeable heads (Figure 3.7). The device’s aim is to serve as an alternative for velocity measurement in AUVs. The hardware used inside the prototype consists of two differential pressure sensors (± 2000 Pa MPXV7002) that are amplified by a 16-bits A/D converter (LTC1867) and 9 degrees of freedom inertial measurement unit (BNO055). Despite the apparent large dimensions of the device, due to the small size of the pressure sensors, the design and dimensions can easily be adapted to cover an expanded range of vehicle sizes and sensor head geometries.

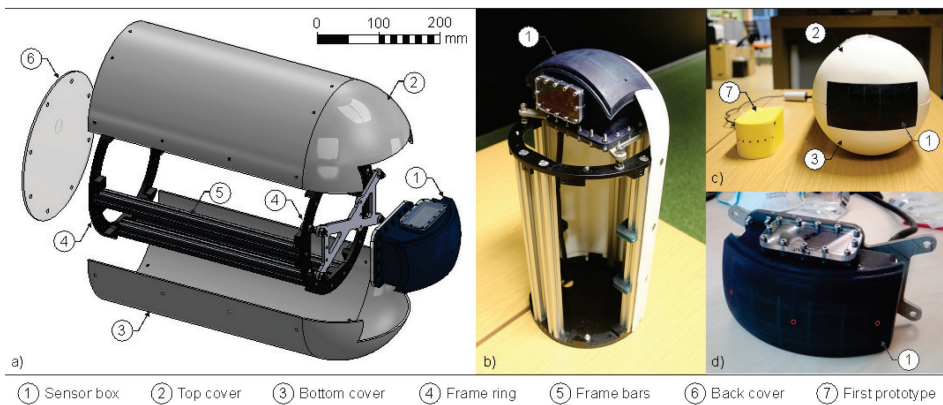


Figure 3.7. First version of the DPSS [82]. a) CAD design of the prototype. b) Side view of the real prototype. c) Comparison of the current platform against the static lab platform used for the preliminary results. d) Sensor box with pressure holes in red.

3.4. Summary and conclusions

The new design concept developed, contrary to the absolute pressure sensor-based ALLs, seems to provide accurate estimations with a high sampling rate, allowing its application in real-time tasks. Similarly, due to the principles of differential pressure sensing, the same sensor can be used for different target depths.

We have also encountered some limitations; for instance, the offset that is generated when the sensor is deployed in water. This issue must be considered differently in each application.

The result of this first laboratory prototype (B-Box) has stimulated the development of other field prototypes. The research area is still open and is mainly focused on the field applicability of the technology. In Chapter 4, the field applicability is analyzed and discussed by means of concrete examples. For these, two main prototypes are used: iRon (the NACA shape prototype shown in *Figure 3.6*) and DPSS (the torpedo shape prototype in *Figure 3.7*). Both prototypes are part of ongoing projects at the Centre for Biorobotics.

4. Applications of differential pressure sensor-based ALLs

The main goal of this research work was to provide methodologies and tools to allow the use of ALLs in diverse real-work applications. For this, it was concluded that classical absolute pressure sensor-based ALLs may suffer from some limitations. Therefore, differential pressure sensor-based artificial lateral lines were developed.

The different prototypes developed (Chapter 3) have been successfully applied in field-oriented research works and have answered questions in fish behavioral studies as well as cover technological gaps in underwater robotic science.

The following chapter summarizes the most relevant works performed with this technology. These works have been distributed in two groups according to their target application as well as the funding projects: 4.1 Underwater speedometry (Robocademy) and 4.2 Fish preferences (BONUS Fishview).

4.1. Underwater velocity estimation

The exploitation of the sensing capabilities of ALLs to perform localization of underwater vehicles can constitute an interesting alternative under structured environments (Section 2.5); regardless, this is subject to the availability of *a priori* maps [35], [39], [107] (Appendix 7). However, a more interesting alternative is presented by the exploitation of hydrodynamic sensing to collect information about the current state of the robot, for instance, to design obstacle avoidance protocols [61] or for velocity estimation to perform navigation [62], [82] (Appendix 8).

The application of a differential pressure sensor-based ALL to estimate the velocity of an underwater vehicle would offer certain advantages in comparison to currently available technology (i.e. DVL [108]–[110] and acoustic Doppler profilers (ADCP) [111]). For instance, hydroacoustic-based systems are expensive, possess a large form factor, and have high energy consumption. For these reasons, they may not be suitable for use in small vehicles [45] or the developing market of low-cost vehicles [46].

Considering this technological gap and our previous laboratory results [62] (Appendix 5), a field-ready platform was developed to validate differential pressure sensor velocity estimation as a viable full-scale technology in autonomous underwater vehicles (AUV). A complete description of the development of the prototype can be found in [82] (Appendix 8). *Figure 4.1* shows the differential pressure sensor speedometer (DPSS) developed for use in torpedo-shaped underwater vehicles (e.g. Sparus II [112]).

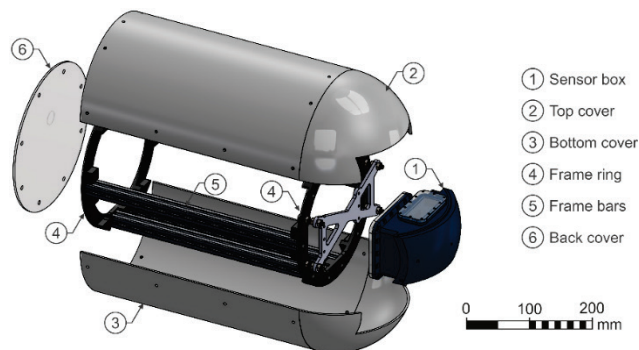


Figure 4.1. DPSS for torpedo-shaped underwater vehicles.

The prototype was tested using two different electronic configurations (*Table 3.1*) and validated using a marine tow tank at the Small Craft Competence Centre in Kuressaare (Saaremaa, Estonia) under variable velocity (0–2 m/s) and acceleration conditions (0–2 m/s²) before its real field test (*Table 4.1*). The first velocity replicate was used for test and calibration while the other velocity replicate and both acceleration replicates were used for validation.

Table 4.1. Conducted experiments. In each test, the target variable (velocity or acceleration) was held constant.

Variables	Replicates	Tow tank carriage settings	Number of experiments
v (m/s)	2	[0.01, 0.05] every 0.01 m/s	64
		[0.10, 0.50] every 0.10 m/s	
		[0.75, 1.00] every 0.25 m/s	
a (m/s ²)	2	[0.01, 0.05] every 0.01 m/s ²	68
		[0.075]	
		[0.10, 0.50] every 0.10 m/s ²	
		[0.75, 1.00] every 0.25 m/s ²	

Figure 4.2 shows the result of the tested acceleration conditions after the independent calibration process. The results demonstrate DPSS's capability to correctly estimate the variable velocities of the carriage with an effective sampling rate higher than 10 Hz.

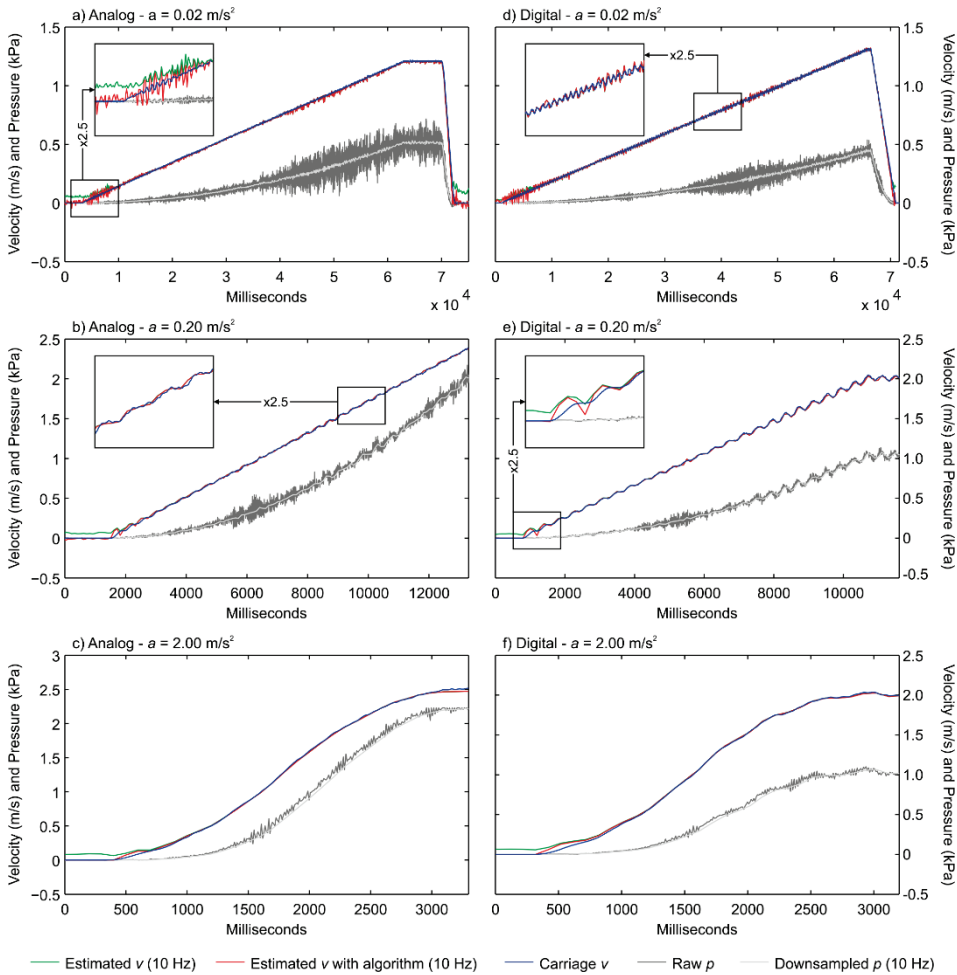


Figure 4.2. Time series analysis of the velocity estimation in three scenarios for two electronic configurations studied (Table 3.1) [82]. Analog sensor: a) Acceleration of 0.02 m/s^2 , deceleration of 0.5 m/s^2 , and detail of the correction algorithm performance, b) Acceleration of 0.20 m/s^2 and detail of velocity oscillation tracking, c) Acceleration of 2.00 m/s^2 . Digital sensor: d) Acceleration of 0.02 m/s^2 , deceleration of 0.3 m/s^2 , and detail of velocity oscillation tracking, e) Acceleration of 0.20 m/s^2 and detail of the correction algorithm performance, f) Acceleration of 2.00 m/s^2 .

The major limitations of the DPSS are as follows:

1. The need to calculate the constant offset (Chapter 3) after each deployment in water for a more accurate estimation of the velocity.
2. The estimation of one-dimensional velocity (in contrast to the three-dimensional vector provided by the DVL or ADCP).
3. In contrast to the DVL to-date, it is not possible to differentiate AUV velocity from water current velocity (as with ADCP).

However, (1) the offset calculation can be implemented in the AUV before the mission starts; (2) further implementation of the prototype may lead to a higher dimensional velocity estimation; and (3) in contrast to DVL, there is no need for bottom tracking for

velocity estimation. Therefore, the technology presents high interest for applications when the use of hydroacoustic devices is not possible (applications limited by size and cost) and is complementary to other technologies (e.g. redundancy or current estimation).

The final objective of the DPSS was its use in a real AUV; the tests were performed during the spring of 2017 (*Figure 4.3*). These results validated the use of DPSS in real-world robotic application; these results are submitted for publication and will not be covered in this thesis.

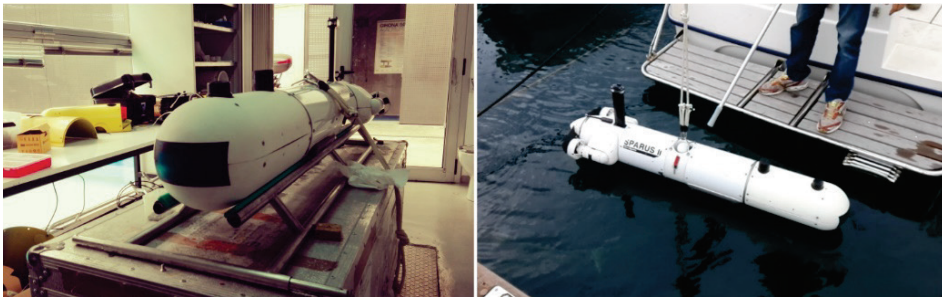


Figure 4.3. DPSS installed in Sparus II [112]; Preparation to perform final experiments.

4.2. Fish preferences

Sometimes, mimicking animal and biological processes may facilitate an understanding of their functioning. Therefore, the bioinspired nature of ALLs can be useful to analyze fish's behavior, sensing capabilities, and preferences. The first ALL that attempted to exploit this principle (Chapter 2) was developed in the BONUS Fishview project. The results using this device were promising but limited due to the drawback of absolute pressure sensors. This motivated the design of iRon, the first differential pressure sensor-based artificial lateral line probe (*Figure 3.6*).

Now, several open works try to correlate iRon's sensor measurements with fish behavior and hydraulic preferences. In this section, we will cover as example the ongoing research on the spatial preferences of Iberian barbel (*Luciobarbus bocagey*) in fishways [85].

The study and analysis of fish habitat preferences is usually based on the point measurements of the physical environment (e.g. time averaged velocity, water depth, substrate type, and underwater vegetation presence). This discretization may lead to an oversimplification of the hydrodynamic characteristics of the aquatic environment, mainly because these metrics (1) ignore the physical interactions between variables and (2) lack the temporal rate and the spatial scale at which fish experience the hydrodynamic stimuli.

The artificial lateral lines sensing capabilities seem to be closer to the fish's perspective when compared to the common techniques used for the measurement of flow hydrodynamic characteristics (e.g. ADV, propellers, etc.). ALLs perform as an all-in-one tool able to (1) perform simultaneous measurement distributed in space, (2) consider the interaction of the fluid with the body of the ALL (spatially distributed sensing) and the surrounding underwater environment (e.g. rocks, plants, walls, etc.), and (3) measure in a sampling rate higher than other field tools and in the same range of

the fish lateral line system. This may explain why ALLs have been successfully used to estimate hydrodynamic variables [13], [22], [23], [26] as well as to identify underwater objects and structures [31].

To test our hypothesis that ALLs could characterize better the variability of the fish spatial selection, the distribution of the barbel in a fishway pool under different hydrodynamic scenarios was monitored. Afterwards, the observed fish positions were modeled using hydrodynamic variables from the LLP as well as variables from a ADV for comparison.

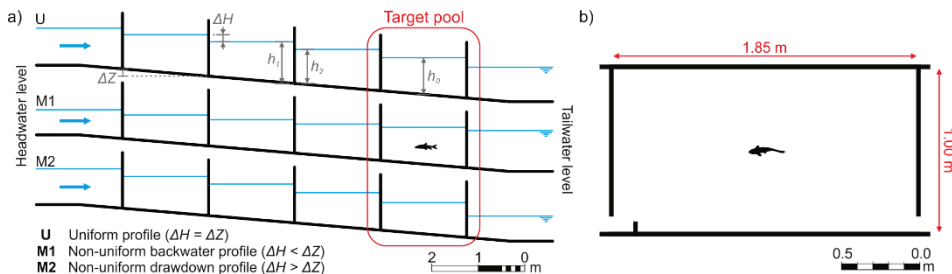
Fishways are structures installed in river obstacles (e.g. dams or weirs) that connect the upstream headwater and downstream tailwater portions of rivers (Figure 4.4). They consist of a sloped channel divided by cross-walls into a series of pools that divide the overall drop into several smaller drops, making the fish passage possible.



Figure 4.4. Example of a fishway. La Flecha, Spain.

Under different headwater and tailwater conditions, fishways will present different hydrodynamics (i.e. different flow structure, velocities or turbulence levels) inside them, in turn, affecting the conditions that fish need to face and, therefore, potentially modifying their behavior and spatial selection.

An indoor vertical slot fishway was selected to perform the experiments. Figure 4.5 and Figure 4.6 illustrate the three scenarios considered as well as the target pool studied. The reader is referred to [85], [113] for more details of the experimental facility and setup.



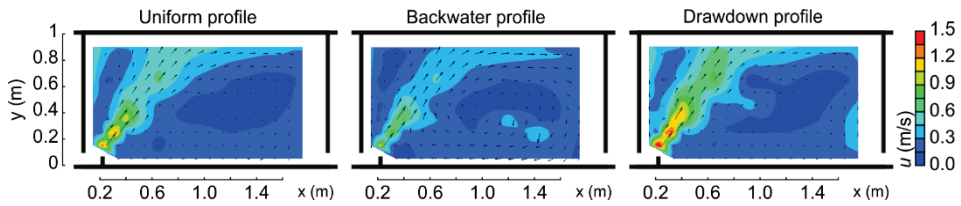


Figure 4.6. Example of differences in flow structure measured with ADV between different hydrodynamic scenarios in the second pool starting from downstream of the structure represented in Figure 4.5 (modified from [85]).

In the past, fish's spatial preferences in fishways were evaluated through widely used hydrodynamic variables, such as velocity, Reynold stress (τ_{xy}), turbulent kinetic energy (TKE), or turbulent intensity (TI) [36], [114]–[116]. These approaches have demonstrated a correlation with fish distribution and preferences; thus, they are generally used for environmental monitoring and assessment. The predictability of these variables was considered as a benchmark, and they were measured with a Vectrino 3D ADV (Nortek AS) (25 Hz).

ALL raw pressure readings were combined to generate different meaningful variables, i.e., correlated with fish presence and interpretable. *Table 4.2* summarizes the final variables selected. Frequency domain variables were left out of this study.

Table 4.2. Pressure-based variables from LLP measurements. Where i is the sensor number, j the position of one value in the data string recorded with the LLP, and N the number of values in the signal string. All pressure (p) units in Pascals.

Variables	Equation
Mean pressure*	$\bar{p}_i = \frac{\sum_{j=1}^n p_{i,j}}{N}$
Mean fluctuations*	$\bar{p}'_i = \frac{\sum_{j=1}^n p_{i,j} - \bar{p}_i }{N}$
Mean front pressure	$\bar{p}_{12} = \frac{\sum_{j=1}^n \frac{p_{1,j} + p_{2,j}}{2}}{N}$
Mean pressure	$\bar{p}_{1-6} = \frac{\sum_{j=1}^n \frac{\sum_{i=1}^6 p_{i,j}}{6}}{N}$
Mean front fluctuations	$\bar{p}'_{12} = \frac{\bar{p}'_1 + \bar{p}'_2}{2}$
Mean fluctuations	$\bar{p}'_{1-6} = \frac{\sum_{j=1}^6 \bar{p}'_j}{6}$
Mean front pressure asymmetry	$\Delta \bar{p}_{12} = \frac{\sum_{j=1}^n (p_{1,j} - p_{2,j})^2}{N}$
Mean pressure asymmetry	$\Delta \bar{p}_{1-6} = \frac{\sum_{j=1}^3 \frac{\sum_{i=1}^n (p_{2i-1,j} - p_{2i,j})^2}{N}}{3}$
Mean front fluctuations asymmetry	$\Delta \bar{p}'_{12} = \frac{\sum_{j=1}^n (p'_{1,j} - p'_{2,j})^2}{N}$
Mean fluctuations asymmetry	$\Delta \bar{p}'_{1-6} = \frac{\sum_{j=1}^3 \frac{\sum_{i=1}^n (p'_{2i-1,j} - p'_{2i,j})^2}{N}}{3}$

*Only for the variable definition above; Sensors are not considered individually.

The relevance of these variables has also been tested for another species, apart from the Iberian barbel, with different ecological traits, e.g. the Japanese eight-barbel loach (*Lefua echigonia*). In both cases, results demonstrated a good agreement of the ALL data with fish distribution or preference.

Five fish were tracked in each scenario (15 fish in total). Their behavior within the pool was monitored continuously through two GoPro cameras on the side and on top of the

pool (Figure 4.5b). The synchronized side-top videos were used to situate the fish inside a 3D-structured grid obtaining a data stream of fish positions referenced to the 3D grid. The fish spatial usage was summed up per prism in the grid to obtain the fish counts of each one. In the same way, the ADV and ALL variables were averaged to the same 3D structured grid. Reader is referred to [85] for a deeper explanation of the methodology.

To test the significance of the hydraulic variables in the fish spatial selection, generalized linear models (GLM) were used. The spatial distribution of fish inside the pool was found to follow an over-dispersed Poisson distribution, and so, a zero inflated Poisson model was applied.

Model selection was performed through a two-step procedure. First, the highly correlated variables were eliminated to reduce multicollinearity. For this, a Spearman correlation threshold of > 0.75 was used. Next, the model selection was made only considering significant variables (p -value < 0.05). In addition to the hydrodynamic variables, two more variables were added to the analysis: the number of walls associated with each 3D volumes (Wall: 0, 1, 2 or 3) and tested scenarios (Case: U, M1 or M2, Figure 4.5) as categorical variables. Table 4.3 summarizes the final models obtained for the ADV and the ALL data.

Table 4.3. Zero-inflated model using ALL and ADV [85].

Model	R ²	MSE	AIC
ALL			
Poisson ($Y \geq 1$): $\text{Log}(Y) = 1 + \text{Wall} * \bar{p}_{1-6} + \text{Wall} * \bar{p}'_{1-6} + \text{Wall} * \text{Case} + \bar{p}_{12} * \text{Case}$	0.817	304.994	4550.94
Binomial ($Y < 1$): $\text{Log}(Y) = 1 + \bar{p}_{1-6} + \bar{p}'_{1-6} + \text{Wall} + \text{Case}$			
ADV			
Poisson ($Y \geq 1$): $\text{Log}(Y) = 1 + TKE + \text{Wall} * \tau_{xy} + \bar{u} * \tau_{xy} + \text{Wall} * \text{Case}$	0.585	687.500	4838.47
Binomial ($Y < 1$): $\text{Log}(Y) = TKE + \text{Wall} + \text{Case} + \bar{u}$			
Y: Number of observed fish in a certain position; Wall: number of walls in a certain position; Case: variable defining the hydraulic conditions.			

It is possible to see that the model generated by the ALL outperforms the ADV model. This might have happened not only because of the higher spatial dimensionality of the ALL (point vs body) but also because of the differences in temporal resolution (25 Hz vs 200 Hz). iRon's distributed sensing capability and its sampling rate make it possible to detect the complex spatial structures found in large-scale turbulent flows as well as wall-body gradients, which are difficult to detect using other point measuring devices. However, further studies are necessary to confirm these results and to establish more direct relations between body fluid pressure interaction and fish preferences.

4.3. Summary and conclusions

The different problem-solving examples presented demonstrate the different possibilities offered by ALL technology as well as the performance of the technology and algorithms developed in Chapter 3.

The lateral lines can be used to perform complex tasks; nevertheless, each task will require slightly different ALL configurations. While we only needed a couple of sensors facing the flow to estimate velocity, the presence of more sensors will allow better discrimination and characterization of the environment. This is useful to perform more complex tasks, such as localization or preference studies.

Regarding underwater speedometry, we can conclude that the speedometry using differential pressure sensors is practical. The performed tests have provided results that validate this technology. However, it is possible to further develop it by increasing the number of sensors to estimate the velocity components and to exploit the distributed sensing capabilities as well as to design an all-in-one navigation system.

In the case of fish preference results, these seem promising. However, more study cases are necessary as the current methodologies for fish preference and habitat modelling are well established in the ecohydraulics community. Thus, despite the results, in order to generate the same amount of data available with the classical approaches will require a tremendous effort. In this regard, the first step should be to validate the variables proposed for the different species and advance in their physical explanation.

Conclusions and future outlook

The aim of this thesis has been to make possible the use of pressure sensor-based ALLs in laboratory and real-world applications, specifically in underwater robotics and underwater environmental studies. The structure of this research has been incremental and multidisciplinary, and the results and conclusions of each chapter have successively defined the following chapter.

First, a detailed study of the current state-of-the-art of ALLs was performed, which resulted in the finding that gauge and absolute pressure sensors have been the most popular sensors used in ALLs. Furthermore, it was found that their usage is motivated by (1) the accessibility of pressure sensors, (2) their reliability, (3) their low cost, (4) their tested performance in other underwater application, and (5) the direct relations of pressure with some flow properties. These characteristics allow the rapid development of new prototypes in comparison with bespoke sensors. However, the review also revealed that the application of gauge and absolute pressure sensor-based ALLs have been limited to laboratory setups, considering ideal hydrodynamic conditions.

After identifying the state of the art and key gaps in ALL implementation, the second step of this work consisted of a study of the classical approaches using this technology. This study revealed that absolute pressure sensor-based ALLs suffer from some limitations that made their application in the real world challenging [50]. Therefore, new methods were proposed for hydrodynamic variable estimation, considering diverse scenarios. These are: (1) a mixed approach [50], (2) statistical approaches [49], [51], and (3) neural network approach [1]. Each of the methods attempt to bypass the limitations using alternative features and they successfully demonstrate their performance under independent validation tests. Using the new features and methods, it is possible to obtain an accurate estimate of velocity and turbulence (R^2 from 0.837 to 0.911 absolute errors from 0.07 to 0.11 m/s for velocity estimates). In the same way, the mixed approach has been successfully applied to define a conceptual application of ALLs in map-based localization problems for AUVs [39].

However, all the alternative features defined required long sampling durations (10–30 s) for their calculation. Despite the fact that recovering the original sampling rate offline is possible [50], this invalidates the absolute pressure sensor-based ALLs in real-time applications. For this reason, differential pressure sensor-based ALLs are proposed as an alternative. A novel method was proposed, tested and validated for their design and creation [62]. This new class of ALL shows that it is possible to achieve the flow velocity estimation in real time (10 Hz). In the same way, the higher sensitivities improved the estimation of low flow velocities and made possible the detection of smaller flow events. Likewise, the higher replicability of the design principles (in shape, sensors, and methods), when compared to previous technologies, has enabled designing different prototypes using the same working principles (B-Box [62], D-Box [83], [106], iRon [85], [87] or DPSS[82]).

This new technology has been successfully applied in two very different disciplines: underwater robotics and fish ecohydraulics preference studies.

In underwater robotics, the sensor was used for speedometry [62], [82]. Testing in both laboratory and field conditions validated this technology for velocity estimation. It was found to provide a potentially new and cost-effective alternative for devices where it is not possible to use other classical velocity estimation approaches (e.g. DVL) due to

their size or cost or a complement for redundancy or flow current estimation in devices with other velocity estimation technologies.

The results from fish preference analyses also provided encouraging results [85], [87]. The bioinspired nature of the ALLs seems to have the potential to characterize fish preferences better than conventional technologies [85]. However, the current technology used for fish preference assessments has been the benchmark for decades, and, thus, all the gathered information is comparable using those technologies and methods. Therefore, to make the application of ALL beneficial as well as to demonstrate its improved performance, it is necessary to offer case studies that can be used as reference points.

Future outlook

The evolution of artificial lateral lines has only just begun. By demonstrating their applicability in real-world case studies, further research and development is expected. However, some challenges remain:

- **Offset.** The new generation of ALLs developed during Chapter 3 can increase the sensitivity as a result of the use of air pressure sensors. However, to use these sensors, it is necessary to use a tubing system for phase separation. This tubing is open and filled with air; thus, whenever it is deployed into the water, the amount of air inside may change, causing a different offset in the sensors each time. This offset is small, and even though it is not relevant in some applications, for others, such estimation of low velocities is essential.
- The elimination of this offset will be possible using wet/wet sensors that can be directly exposed to the fluid. However, wet/wet sensors with the required sensitivity are currently not commercially available or not available with a suitable housing or design. The best and most interesting alternative is DP86 [117], but this is not as sensitive as the alternative proposed in the thesis (0 to 6894.76 Pa); they are bulky, expensive (224.44€ against 10.67€, eu.mouser.com) and have a shape that is difficult to adapt into our applications. Nevertheless, the technology used in this sensor may give some clues about possible advances in sensors that can be used to develop a new generation of high sensitivity wet/wet sensors.
- **Data fusion.** All the developed prototypes are subject to disturbances not directly related to pressure, such as body fluctuations or sensor body orientations that may generate unwanted pressure fluctuations. Considering these disturbances, the combination of an inertial measurement unit in conjunction with the pressure signals may facilitate the development of a filter algorithm or models that can further improve the performance of the developed ALLs. To develop this, filter tests under controlled environment must be done – first, considering experiment with our disturbances, and, later, under controlled disturbances.
- **Spatial distribution.** To estimate the velocity in Chapter 3, we proposed an optimal distribution of pressure sensors in the front part of the spherical shapes. However, this technology can perform other sensing tasks, such as the detection of walls proposed in [61]. Moreover, with a correct distribution, it may have the potential to estimate all the components of the velocity vector. To achieve this, further research of the sensor distribution over the body is necessary – first, by approaching with simulated models, and later, through controlled experiments.

- **Physics.** To better understand the measurements that we perform with the new differential pressure sensor-based ALLs, it is necessary to develop a controlled experiment as the ones conducted with absolute pressure sensors in past years. This would facilitate our understanding of the variables defined in *Table 4.2* or help developing more significant ones for all the possible applications of the differential pressure sensor-based ALLs.
- **Sensitivity.** Even if we increase the sensitivity, the estimation of low velocities will present problems. Natural underwater environments have many pressure sources that are detected by the pressure sensors. Thus, even if we can make measurements with a high level of sensitivity, low velocities will produce very small pressures that will be masked by those noise sources. This is one of the limitations of pressure sensors that we will need to accommodate.
- **Interdisciplinary collaboration.** As has been observed in the studies conducted, the ALLs applications cover different scientific fields. Therefore, to produce conclusive results, collaboration with other disciplines is necessary. This will allow a better understanding of the technology, allowing for further performance improvements.

References

- [1] J. A. Tuhtan, J. F. Fuentes-Pérez, G. Toming, and M. Kruusmaa, "Flow velocity estimation using a fish-shaped lateral line probe with product-moment correlation features and a neural network," *Flow Meas. Instrum.*, vol. 54, pp. 1–8, Apr. 2017.
- [2] D. E. Dombroski and J. P. Crimaldi, "The accuracy of acoustic Doppler velocimetry measurements in turbulent boundary layer flows over a smooth bed," *Limnol. Oceanogr. Methods*, vol. 5, no. 1, pp. 23–33, 2007.
- [3] N. Mori, T. Suzuki, and S. Kakuno, "Noise of acoustic Doppler velocimeter data in bubbly flows," *J. Eng. Mech.*, vol. 133, no. 1, pp. 122–125, 2007.
- [4] B. J. MacVicar, E. Beaulieu, V. Champagne, and A. G. Roy, "Measuring water velocity in highly turbulent flows: field tests of an electromagnetic current meter (ECM) and an acoustic Doppler velocimeter (ADV)," *Earth Surf. Process. Landforms*, vol. 32, no. 9, pp. 1412–1432, 2007.
- [5] T. M. Hammond, C. B. Pattiaratchi, M. J. Osborne, and M. Collins, "Field and flume comparisons of the modified and standard (Savonius-rotor) Aanderaa self-recording current meters," *Dtsch. Hydrogr. Zeitschrift*, vol. 39, no. 2, pp. 41–63, 1986.
- [6] C. L. Cook and D. J. Coughlin, "Rainbow trout *Oncorhynchus mykiss* consume less energy when swimming near obstructions," *J. Fish Biol.*, vol. 77, no. 7, pp. 1716–1723, 2010.
- [7] Y. Yang *et al.*, "Artificial lateral line with biomimetic neuromasts to emulate fish sensing," *Bioinspir. Biomim.*, vol. 5, no. 1, p. 16001, 2010.
- [8] S. M. van Netten and M. J. McHenry, "The biophysics of the fish lateral line," in *The Lateral Line System*, Springer, 2013, pp. 99–119.
- [9] R. Venturelli *et al.*, "Hydrodynamic pressure sensing with an artificial lateral line in steady and unsteady flows," *Bioinspir. Biomim.*, vol. 7, no. 3, p. 36004, 2012.
- [10] N. Chen, J. Chen, J. Engel, S. Pandya, C. Tucker, and C. Liu, "Development and characterization of high sensitivity bioinspired artificial haircell sensor," *Proc. Solid-State Sensors, Actuators, Microsystems Work.*, 2006.
- [11] A. Klein and H. Bleckmann, "Determination of object position, vortex shedding frequency and flow velocity using artificial lateral line canals," *Beilstein J. Nanotechnol.*, vol. 2, no. 1, pp. 276–283, 2011.
- [12] A. T. Abdulsadda and X. Tan, "An artificial lateral line system using IPMC sensor arrays," *Int. J. Smart Nano Mater.*, vol. 3, no. 3, pp. 226–242, 2012.
- [13] T. Salumäe and M. Kruusmaa, "Flow-relative control of an underwater robot," *Proc. R. Soc. A Math. Phys. Eng. Sci.*, vol. 469, no. 2153, p. 20120671, 2013.
- [14] Y. Yang, N. Chen, C. Tucker, J. Engel, S. Pandya, and C. Liu, "From artificial hair cell sensor to artificial lateral line system: development and application," in *IEEE 20th International Conference on Micro Electro Mechanical Systems, MEMS 2007*, 2007, pp. 577–580.
- [15] J. J. Van Baar, M. Dijkstra, R. J. Wiegerink, T. S. J. Lammerink, and G. J. M. Krijnen, "Fabrication of arrays of artificial hairs for complex flow pattern recognition," in *Sensors, 2003. Proceedings of IEEE*, 2003, vol. 1, pp. 332–336.
- [16] A. M. K. Dagamseh, C. M. Bruinink, H. Droogendijk, R. J. Wiegerink, T. S. J. Lammerink, and G. J. M. Krijnen, "Engineering of biomimetic hair-flow sensor arrays dedicated to high-resolution flow field measurements," in *Sensors, 2010 IEEE*, 2010, pp. 2251–2254.

- [17] A. G. P. Kottapalli, M. Asadnia, J. M. Miao, G. Barbastathis, and M. S. Triantafyllou, "A flexible liquid crystal polymer MEMS pressure sensor array for fish-like underwater sensing," *Smart Mater. Struct.*, vol. 21, no. 11, p. 115030, 2012.
- [18] V. I. Fernandez, S. M. Hou, F. S. Hover, J. H. Lang, and M. S. Triantafyllou, "Development and application of distributed MEMS pressure sensor array for AUV object avoidance," Massachusetts Institute of Technology. Sea Grant College Program, 2009.
- [19] J. Chen, J. Engel, N. Chen, S. Pandya, S. Coombs, and C. Liu, "Artificial lateral line and hydrodynamic object tracking," in *19th IEEE International Conference on Micro Electro Mechanical Systems, MEMS 2006*, 2006, pp. 694–697.
- [20] Y. Yang *et al.*, "Distant touch hydrodynamic imaging with an artificial lateral line," *Proc. Natl. Acad. Sci. U. S. A.*, vol. 103, no. 50, pp. 18891–18895, 2006.
- [21] A. T. Abdulsadda and X. Tan, "Underwater source localization using an IPMC-based artificial lateral line," in *IEEE International Conference on Robotics and Automation, ICRA 2011*, 2011, pp. 2719–2724.
- [22] L. DeVries, F. D. Lagor, H. Lei, X. Tan, and D. A. Paley, "Distributed flow estimation and closed-loop control of an underwater vehicle with a multi-modal artificial lateral line," *Bioinspir. Biomim.*, vol. 10, no. 2, p. 25002, 2015.
- [23] V. I. Fernandez, "Performance analysis for lateral-line-inspired sensor arrays," DTIC Document, 2011.
- [24] J. Ježov, *Pressure sensitive lateral line for underwater robot*. Tallinn: TUT Press, 2013.
- [25] T. Salumäe, *Flow-sensitive Robotic Fish: From Concept to Experiments*. Tallinn: TUT Press, 2015.
- [26] M. Kruusmaa, G. Toming, T. Salumae, J. Jezov, and A. Ernits, "Swimming speed control and on-board flow sensing of an artificial trout," in *IEEE International Conference on Robotics and Automation, ICRA 2011*, 2011, pp. 1791–1796.
- [27] W. Wang, Y. Li, X. Zhang, C. Wang, S. Chen, and G. Xie, "Speed Evaluation of a Freely Swimming Robotic Fish with an Artificial Lateral Line," in *IEEE International Conference on Robotics and Automation, ICRA 2016*, 2016, pp. 1–6.
- [28] V. I. Fernandez, A. Maertens, F. M. Yaul, J. Dahl, J. H. Lang, and M. S. Triantafyllou, "Lateral-line-inspired sensor arrays for navigation and object identification," *Mar. Technol. Soc. J.*, vol. 45, no. 4, pp. 130–146, 2011.
- [29] L. D. Chambers *et al.*, "A fish perspective: detecting flow features while moving using an artificial lateral line in steady and unsteady flow," *J. R. Soc. Interface*, vol. 11, no. 99, p. 20140467, 2014.
- [30] W. Wang, X. Zhang, J. Zhao, and G. Xie, "Sensing the neighboring robot by the artificial lateral line of a bio-inspired robotic fish," in *Intelligent Robots and Systems (IROS), 2015 IEEE/RSJ International Conference on*, 2015, pp. 1565–1570.
- [31] N. Muhammad, N. Strokina, G. Toming, J. Tuhtan, J. K. Kämäräinen, and M. Kruusmaa, "Flow feature extraction for underwater robot localization: preliminary results.," in *IEEE International Conference on Robotics and Automation, ICRA 2015*, 2015, pp. 1125–1130.
- [32] J. Tuhtan, N. Strokina, G. Toming, N. Muhammad, M. Kruusmaa, and J.-K. Kämäräinen, "Hydrodynamic classification of natural flows using an artificial lateral line and frequency domain feature.," in *IAHR World Congress*, 2015.

- [33] T. Salumäe, I. Ranó, O. Akanyeti, and M. Kruusmaa, "Against the flow: A Braitenberg controller for a fish robot," in *IEEE International Conference on Robotics and Automation, ICRA 2012*, 2012, pp. 4210–4215.
- [34] X. Zheng, C. Wang, R. Fan, and G. Xie, "Artificial lateral line based local sensing between two adjacent robotic fish," *Bioinspir. Biomim.*, vol. 13, no. 1, p. 16002, 2017.
- [35] N. Muhammad, G. Toming, J. A. Tuhtan, M. Musall, and M. Kruusmaa, "Underwater map-based localization using flow features," *Auton. Robots*, vol. 41, no. 2, pp. 417–436, 2017.
- [36] A. T. Silva, J. M. Santos, M. T. Ferreira, A. N. Pinheiro, and C. Katopodis, "Effects of water velocity and turbulence on the behaviour of Iberian barbel (*Luciobarbus bocagei*, Steindachner 1864) in an experimental pool-type fishway," *River Res. Appl.*, vol. 27, pp. 360–373, 2011.
- [37] N. Lamouroux, H. Capra, M. Pouilly, and Y. Souchon, "Fish habitat preferences in large streams of southern France," *Freshw. Biol.*, vol. 42, no. 4, pp. 673–687, 1999.
- [38] A. Gao and M. Triantafyllou, *Bio-inspired pressure sensing for active yaw control of underwater vehicles*. IEEE, 2012.
- [39] J. F. Fuentes-Pérez *et al.*, "Map-based localization in structured underwater environment using simulated hydrodynamic maps," in *IEEE ROBIO 2017*, 2017.
- [40] K. Streitlien, G. S. Triantafyllou, and M. S. Triantafyllou, "Efficient foil propulsion through vortex control," *Aiaa J.*, vol. 34, no. 11, pp. 2315–2319, 1996.
- [41] D. S. Barrett, M. S. Triantafyllou, D. K. P. Yue, M. A. Grosenbaugh, and M. J. Wolfgang, "Drag reduction in fish-like locomotion," *J. Fluid Mech.*, vol. 392, pp. 183–212, 1999.
- [42] M. Sfakiotakis, D. M. Lane, and J. B. C. Davies, "Review of fish swimming modes for aquatic locomotion," *IEEE J. Ocean. Eng.*, vol. 24, no. 2, pp. 237–252, 1999.
- [43] Ø. Hegrenæs and E. Berglund, "Doppler Water-Track Aided Inertial Navigation for Autonomous Underwater Vehicle," in *OCEANS 2009 - EUROPE*, 2009, pp. 1–10.
- [44] R. McEwen, H. Thomas, D. Weber, and F. Psota, "Performance of an AUV navigation system at arctic latitudes," *IEEE J. Ocean. Eng.*, vol. 30, no. 2, pp. 443–454, 2005.
- [45] T. Salumäe *et al.*, "Design principle of a biomimetic underwater robot U-CAT," 2014, pp. 1–5.
- [46] O. A. Viquez, E. M. Fischell, N. R. Rypkema, and H. Schmidt, "Design of a General Autonomy Payload for Low-Cost AUV R & D," in *IEEE/OES AUV*, 2016, pp. 151–155.
- [47] D. L. Rudnick, R. E. Davis, C. C. Eriksen, D. M. Fratantoni, and M. J. Perry, "Underwater gliders for ocean research," *Mar. Technol. Soc. J.*, vol. 38, no. 2, pp. 73–84, 2004.
- [48] C. Wang, W. Wang, and G. Xie, "Speed estimation for robotic fish using onboard artificial lateral line and inertial measurement unit," in *2015 IEEE ROBIO*, 2015, pp. 285–290.
- [49] K. Chen *et al.*, "Estimation of flow turbulence metrics with a lateral line probe and regression," *IEEE Trans. Instrum. Meas.*, vol. 66, no. 4, pp. 651–660, 2017.
- [50] J. F. Fuentes-Pérez *et al.*, "Current velocity estimation using a lateral line probe," *Ecol. Eng.*, vol. 85, pp. 296–300, 2015.

- [51] N. Strokina, J.-K. Kamarainen, J. A. Tuhtan, J. F. Fuentes-Pérez, and M. Kruusmaa, "Joint Estimation of Bulk Flow Velocity and Angle Using a Lateral Line Probe," *Instrum. Meas. IEEE Trans.*, vol. 65, no. 3, 2016.
- [52] S. Coomb, P. Görner, and H. Munz, *Mechanosensory Lateral Line System*. Springer Science & Business Media, 2012.
- [53] S. Coombs, C. B. Braun, and B. Donovan, "The orienting response of Lake Michigan mottled sculpin is mediated by canal neuromasts," *J. Exp. Biol.*, vol. 204, no. Pt 2, pp. 337–348, 2001.
- [54] E.-S. Hassan, H. Abdel-Latif, and R. Biebricher, "Studies on the effects of Ca² and Co on the swimming behavior of the blind Mexican cave fish," *J. Comp. Physiol. A*, vol. 171, no. 3, pp. 413–419, 1992.
- [55] J. C. Montgomery, C. F. Baker, and A. G. Carton, "The lateral line can mediate rheotaxis in fish," *Nature*, vol. 389, no. 6654, pp. 960–963, 1997.
- [56] T. J. Pitcher, B. L. Partridge, and C. S. Wardle, "A blind fish can school," *Science*, vol. 194, no. 4268, pp. 963–965, 1976.
- [57] S. Dijkgraaf, "The functioning and significance of the lateral-line organs," *Biol. Rev.*, vol. 38, no. 1, pp. 51–105, 1963.
- [58] S. P. Windsor and M. J. McHenry, "The influence of viscous hydrodynamics on the fish lateral-line system," *Integr. Comp. Biol.*, vol. 49, no. 6, pp. 691–701, 2009.
- [59] Z. Fan, J. Chen, J. Zou, D. Bullen, C. Liu, and F. Delcomyn, "Design and fabrication of artificial lateral line flow sensors," *J. Micromechanics Microengineering*, vol. 12, no. 5, p. 655, 2002.
- [60] K. Nelson and K. Mohseni, "An artificial fish lateral line sensory system composed of modular pressure sensor blocks," in *Robotics and Automation (ICRA), 2017 IEEE International Conference on*, 2017, pp. 4914–4919.
- [61] Y. Xu and K. Mohseni, "A Pressure Sensory System Inspired by the Fish Lateral Line: Hydrodynamic Force Estimation and Wall Detection," *IEEE J. Ocean. Eng.*, 2016.
- [62] J. F. Fuentes-Pérez, K. Kalev, J. A. Tuhtan, and M. Kruusmaa, "Underwater vehicle speedometry using differential pressure sensors: Preliminary results," in *IEEE/OES AUV*, 2016, p. 6.
- [63] J. Ježov, O. Akanyeti, L. D. Chambers, and M. Kruusmaa, "Sensing oscillations in unsteady flow for better robotic swimming efficiency," in *Systems, Man, and Cybernetics (SMC), 2012 IEEE International Conference on*, 2012, pp. 91–96.
- [64] J. A. Tuhtan *et al.*, "Man-made flows from a fish's perspective: autonomous classification of turbulent fishway flows with field data collected using an artificial lateral line," *Bioinspir. Biomim.*, 2018.
- [65] O. Akanyeti *et al.*, "Self-motion effects on hydrodynamic pressure sensing: part I. Forward–backward motion," *Bioinspir. Biomim.*, vol. 8, no. 2, p. 26001, 2013.
- [66] Tradesparq, "MS5540C Pressure Sensor Miniature Barometer Module," 2018. [Online]. Available: <http://www.tradesparq.com/products/2299461/MS5540C-Pressure-Sensor-Miniature-Barometer-Module-manufacturers>.
- [67] E. J. Denton and J. A. B. Gray, "Mechanical factors in the excitation of the lateral lines of fishes," in *Sensory biology of aquatic animals*, Springer, 1988, pp. 595–617.
- [68] J. A. Tuhtan *et al.*, "Design and application of a fish-shaped lateral line probe for flow measurement," *Rev. Sci. Instrum.*, vol. 045110, no. 4, pp. 1–8, 2016.

- [69] J. A. Tuhtan, J. F. Fuentes-Pérez, G. Toming, M. Schneider, and M. Schletterer, "A fish is not a point: Analyses of innatura hydrodynamic signatures in fish migration facilities, using a fish-shaped lateral line probe," *WasserWirtschaft*, vol. 108, no. 2–3, pp. 48–53, 2018.
- [70] D. Xu, H. Zeng, J. Liu, and J. Wang, "Hydrodynamic analysis with an artificial lateral line of robotic fish," in *Industrial Electronics and Applications (ICIEA), 2017 12th IEEE Conference on*, 2017, pp. 1380–1385.
- [71] M. Ji, Y. Zhang, X. Zheng, G. Liu, and J. Qiu, "A fish-shaped minimal prototype of lateral line system based on pressure sensing," in *Mechatronics and Automation (ICMA), 2017 IEEE International Conference on*, 2017, pp. 596–601.
- [72] X. Zheng *et al.*, "Underwater Positioning Based on an Artificial Lateral Line and a Generalized Regression Neural Network," *J. Bionic Eng.*, vol. 15, no. 5, pp. 883–893, 2018.
- [73] G. Liu *et al.*, "Research on Flow Field Perception Based on Artificial Lateral Line Sensor System," *Sensors*, vol. 18, no. 3, p. 838, 2018.
- [74] FistSensor, "Understanding the difference between absolute, gage and differential pressure," 2017. [Online]. Available: <https://www.first-sensor.com/en/products/pressure-sensors/pressure-sensors-and-transmitters/pressure-types.html>.
- [75] E. Ower and R. C. Pankhurst, *The measurement of air flow*. Elsevier, 2014.
- [76] A. H. Glaser, "The pitot cylinder as a static pressure probe in turbulent flow," *J. Sci. Instrum.*, vol. 29, no. 7, p. 219, 1952.
- [77] K. H. Beij, "Aircraft Speed Instruments," 1933.
- [78] E. N. Brown, C. A. Friehe, and D. H. Lenschow, "The use of pressure fluctuations on the nose of an aircraft for measuring air motion," *J. Clim. Appl. Meteorol.*, vol. 22, no. 1, pp. 171–180, 1983.
- [79] J. Hacker and T. Crawford, "The BAT-probe: The ultimate tool to measure turbulence from any kind of aircraft (or sailplane)," *Tech. Soar.*, vol. 23, no. 2, pp. 43–46, 1999.
- [80] K. E. Garman *et al.*, "An Airborne and Wind Tunnel Evaluation of a Wind Turbulence Measurement System for Aircraft-Based Flux Measurements*," *J. Atmos. Ocean. Technol.*, vol. 23, no. 12, pp. 1696–1708, 2006.
- [81] A. Al Makky, "http://cfd2012.com/pitot-tube.html," 2012. [Online]. Available: <http://cfd2012.com/pitot-tube.html>.
- [82] J. F. Fuentes-Pérez *et al.*, "Differential Pressure Sensors for Underwater Speedometry in Variable Velocity and Acceleration Conditions," *IEEE J. Ocean. Eng.*, 2018.
- [83] M. Schletterer, H. Götsch, J. A. Tuhtan, J. F. Fuentes-Pérez, and M. Kruusmaa, "More than depth: developing pressure sensing systems for aquatic environments. More than depth: developing pressure sensing systems for aquatic environments," in *HydroSenSoft, International Symposium and Exhibition on Hydro-Environment Sensors and Software.*, 2017.
- [84] M. J. Costa, J. F. Fuentes-Pérez, I. Boavida, J. A. Tuhtan, and A. N. Pinheiro, "Fish under pressure: examining behavioural responses of Iberian barbel under simulated hydropeaking with instream structures," *PLoS one (Under Rev.)*, 2018.
- [85] J. F. Fuentes-Pérez, M. Eckert, J. A. Tuhtan, M. T. Ferreira, M. Kruusmaa, and P. Branco, "Spatial preferences of Iberian barbel in a vertical slot fishway under variable hydrodynamic scenarios," *Ecol. Eng.*, vol. 125, pp. 131–142, Dec. 2018.

- [86] J. F. Fuentes-Pérez, J. A. Tuhtan, P. Branco, M. Eckert, M. T. Ferreira, and M. Kruusmaa, "A 3D data-driven approach to study the hydrodynamic preferences of fish in fishways," in *International Symposium of Ecohydraulics 2018*, 2018.
- [87] M. J. Costa, J. F. Fuentes-Pérez, I. Boavida, J. A. Tuhtan, and A. N. Pinheiro, "Behaviour responses of Iberian barbel to simulated hydropeaking event: effects of instream structures and fluid body interactions," in *International Symposium of Ecohydraulics 2018*, 2018.
- [88] K. Nelson and K. Mohseni, "Design of a 3-D Printed, Modular Lateral Line Sensory System for Hydrodynamic Force Estimation," *Mar. Technol. Soc. J.*, vol. 51, no. 5, pp. 103–115, 2017.
- [89] S. Pandya, Y. Yang, D. L. Jones, J. Engel, and C. Liu, "Multisensor processing algorithms for underwater dipole localization and tracking using MEMS artificial lateral-line sensors," *EURASIP J. Adv. Signal Process.*, vol. 2006, 2006.
- [90] N. Nguyen, D. L. Jones, Y. Yang, and C. Liu, "Flow vision for autonomous underwater vehicles via an artificial lateral line," *EURASIP J. Adv. Signal Process.*, vol. 2011, p. 9, 2011.
- [91] Q. Zhu, K. Zhong, and G. Xie, "Speed estimation for robotic fish based on pressure sensor," in *Control and Decision Conference (2014 CCDC), The 26th Chinese*, 2014, pp. 2714–2718.
- [92] W. Wang, D. Gu, and G. Xie, "Autonomous Optimization of Swimming Gait in a Fish Robot With Multiple Onboard Sensors," *IEEE Trans. Syst. Man, Cybern. Syst.*, 2017.
- [93] L. Paull, S. S. Saeedi, M. Seto, and H. H. H. Li, "AUV navigation and localization: A review," *Ocean. Eng. IEEE J.*, vol. 39, no. 1, pp. 131–149, 2014.
- [94] D. Bernoulli, *Hydrodynamica: sive de viribus et motibus fluidorum commentarii*. 1738.
- [95] M. Kabaciński and J. Pospolita, "Numerical and experimental research on new cross-sections of averaging Pitot tubes," *Flow Meas. Instrum.*, vol. 19, no. 1, pp. 17–27, 2008.
- [96] A. B. Dubois, G. A. Cavagna, and R. S. Fox, "Pressure distribution on the body surface of swimming fish," *J. Exp. Biol.*, vol. 60, pp. 581–591, 1974.
- [97] J. F. Fuentes-Pérez *et al.*, "3D modelling of non-uniform and turbulent flow in vertical slot fishways," *Environ. Model. Softw.*, vol. 99, 2018.
- [98] J. Wolf, W. Burgard, and H. Burkhardt, "Robust vision-based localization by combining an image-retrieval system with Monte Carlo localization," *Robot. IEEE Trans.*, vol. 21, no. 2, pp. 208–216, 2005.
- [99] A. Huster, S. D. Fleischer, and S. Rock, "Demonstration of a vision-based dead-reckoning system for navigation of an underwater vehicle," in *Autonomous Underwater Vehicles, 1998. AUV'98. Proceedings of the 1998 Workshop on*, 1998, pp. 185–189.
- [100] M. Carreras, P. Ridao, R. García, and T. Nicosevici, "Vision-based localization of an underwater robot in a structured environment," in *IEEE International Conference on Robotics and Automation, ICRA 2003*, 2003, vol. 1, pp. 971–976.
- [101] D. Forouher, J. Hartmann, M. Litza, and E. Maehle, "Sonar-based fastslam in an underwater environment using walls as features," in *Advanced Robotics (ICAR), 2011 15th International Conference on*, 2011, pp. 588–593.

- [102] A. Mallios, P. Ridaou, D. Ribas, M. Carreras, and R. Camilli, "Toward autonomous exploration in confined underwater environments," *J. F. Robot.*, vol. 33, no. 7, pp. 994–1012, 2016.
- [103] O. Akanyeti, P. J. M. Thornycroft, G. V. Lauder, Y. R. Yanagitsuru, A. N. Peterson, and J. C. Liao, "Fish optimize sensing and respiration during undulatory swimming," *Nat. Commun.*, vol. 7, 2016.
- [104] J. D. Anderson Jr, *Fundamentals of aerodynamics*. Tata McGraw-Hill Education, 2010.
- [105] A. K. Gupta, A. K. Gupta, and D. G. Lilley, *Flowfield modeling and diagnostics*, vol. 4. Taylor & Francis, 1985.
- [106] M. Schmidt, J. Tuhtan, and M. Schletterer, "Hydroacoustic and Pressure Turbulence Analysis for the Assessment of Fish Presence and Behavior Upstream of a Vertical Trash Rack at a Run-of-River Hydropower Plant," *Appl. Sci.*, vol. 8, no. 10, p. 1723, 2018.
- [107] N. Muhammad, J. F. Fuentes-Pérez, J. A. Tuhtan, G. Toming, M. Musall, and M. Kruusmaa, "Map-based localization and loop-closure detection from a moving underwater platform using flow features," *Auton. Robots*, pp. 1–16, 2018.
- [108] G. Grenon, P. E. An, S. M. Smith, and A. J. Healey, "Enhancement of the inertial navigation system for the Morpheus autonomous underwater vehicles," *IEEE J. Ocean. Eng.*, vol. 26, no. 4, pp. 548–560, 2001.
- [109] L. Whitcomb and D. Yoerger, "Towards Precision Robotic Maneuvering , Survey , and Manipulation in Unstructured Undersea Environments 1 Introduction," *Dana*, vol. 8, pp. 45–54, 1998.
- [110] B. Jalving, K. Gade, K. Svartveit, A. Willumsen, and R. Sørhagen, "DVL Velocity Aiding in the HUGIN 1000 Integrated Inertial Navigation System," *Model. Identif. Control*, vol. 25, no. 4, pp. 223–235, 2004.
- [111] D. A. Fong and N. L. Jones, "Evaluation of AUV-based ADCP measurements," *Limnol. Oceanogr. methods*, vol. 4, no. 3, pp. 58–67, 2006.
- [112] M. Carreras *et al.*, "Sparus II, design of a lightweight hovering AUV," in *International Workshop on Marine Technology*, 2013.
- [113] J. F. Fuentes-Pérez *et al.*, "Hydraulics of vertical slot fishways: Non-uniform profiles," *J. Hydraul. Eng.*, 2019.
- [114] C. M. Alexandre *et al.*, "Use of electromyogram telemetry to assess the behavior of the Iberian barbel (*Luciobarbus bocagei* Steindachnert, 1864) in a pool-type fishway," *Ecol. Eng.*, vol. 51, pp. 191–202, 2013.
- [115] F. Romão *et al.*, "Passage performance of two cyprinids with different ecological traits in a fishway with distinct vertical slot configurations," *Ecol. Eng.*, vol. 105, pp. 180–188, 2017.
- [116] J. M. Santos *et al.*, "Ecohydraulics of pool-type fishways: getting past the barriers," *Ecol. Eng.*, vol. 48, pp. 38–50, 2012.
- [117] J. N. Moum, "Ocean speed and turbulence measurements using pitot-static tubes on moorings," *J. Atmos. Ocean. Technol.*, vol. 32, no. 7, pp. 1400–1413, 2015.

Acknowledgements

I would like to express my sincere gratitude to my supervisors Professor Maarja Kruusmaa and Dr. Eng. Jeffrey A. Tuhtan. They have given me this opportunity and without their guidance, ideas, support, critical feedback, knowledge and trust this work would not have been possible. Thank you.

I would like to thank all the partners and collaborators involved in this research and especially my colleagues at the Centre for Biorobotics, not only because of everything they have taught me but also because they made the cold and dark winters of Estonia warm and shiny.

The research presented in this thesis was funded by:

- The ROBOCADEMY training and research network (608096) funded by the European Union's Seventh Programme,
- The FISHVIEW project funded from BONUS, the joint Baltic Sea Research and Development Programme (Art 185), funded jointly by the European Union's Seventh Programme for research, technological development and demonstration, and by the Academy of Finland (under the grant 280715), the German Federal Ministry for Education and Research (BMBF FKZ:03F0687A) and the Estonian Environmental Investment Centre (KIK P.7254 C.3255)
- IUT (IUT33-9) institutional research funding of the Estonian Ministry of Education and Research.
- FiThydro project funded by European Union's H2020 research and innovation program under grant agreement No. 727830.
- "Bioinspired flow sensing" Estonian Research Council grant (PUT1690)
- "Octavo" Estonian base financing grant (No. B53).
- The Archimedes Foundation.

Finally, I want to thank my family and friends for always being there for me.

Abstract

Flow Sensing with Pressure Sensor-Based Artificial Lateral Lines: from the Laboratory to the Field

Natural water flows range from the massive ocean currents driven by changes in global winds and temperature to the tiny vortices formed by pebbles in a stream. Accordingly, aquatic organisms have adapted to natural flows by developing an impressive array of underwater sensing techniques. Among the best understood of these advanced biological flow sensing organs is the fish's octavolateralis afferent system, commonly referred to as the "lateral line" because it runs along the sides of the fish's body. The biological lateral line contributes to many different fish behaviors including rheotaxis, schooling, predator and obstacle avoidance and prey localization. Its efficiency and utility under the broad range and complexity of natural flows has inspired researchers to develop the artificial lateral line (ALL). Large-scale implementation of ALLs can provide new ways of measuring and classifying natural water flows, provide insights into the physical characteristics of aquatic habitats and improve the sensing abilities of underwater robots. However, the current applications of ALLs have been limited to laboratory conditions.

The aim of this thesis is to free the ALL from the laboratory, creating a new type of field-ready ALL which can be used in environmental studies and in underwater robotics. Consequently, this thesis is a highly multidisciplinary work at the frontier of robotics, bioinspired flow sensing, ecology and hydraulics. The aim has been achieved in three steps, following an incremental development.

In the first step (Chapter 2), a state-of-the-art absolute pressure sensor based ALL was studied. The evaluation of ALL performance revealed critical limitations for its use in real-world conditions. To overcome these limitations, new algorithms and semi-empirical relations to estimate water flow variables (water velocity and turbulence) were experimentally determined. These new methods, in contrast to existing ALL approaches, provide accurate estimations of the variables independently of calibration procedures, including angular deviations of the ALL. The newly developed algorithms and relations enable the ALL to function under a broader spectrum of hydrodynamic conditions, including field measurements. However, a major drawback of the achievements of the first research step is the requirement that the data be evaluated in post-processing, prohibiting the use of ALL under real-time conditions.

Real-time state estimation is crucial for ALL applications in underwater robotics, where decisions must be taken in response to a fast-changing environment. Therefore, the second step (Chapter 3) was the development of a new generation of real-time ALLs using a novel method based on high sensitivity air differential pressure sensors. This method overcomes the previous technological constraints suffered by absolute pressure sensors. The differential ALL includes auto-calibration, an improvement in depth-dependent sensitivity as well as the removal of diurnal barometric pressure changes. The output of the second development step was the creation of a real-time, differential ALL. Furthermore, through testing and validation of this new ALL, a generalized empirical relation was produced, capable of providing accurate instantaneous estimates of velocity independent of the angle of attack. A major finding of the second step was that differential, air-based ALLs allow for an improvement in sensitivity of 10,000% over the state-of-the-art total pressure devices used in step 1.

The development of the differential ALL solved the major drawbacks identified in step one using absolute pressure sensors. Therefore, the final step (Chapter 4) consists of real-world applications including calibration, testing and validation. Specifically, two applications were considered (1) real-time velocity estimation for underwater robots and (2) characterization of hydraulic fish preferences in a vertical slot fishway. In both cases, the performance of the proposed ALLs with ground truth datasets was assessed to show their performance and to demonstrate the improvements over the state-of-the-art.

The results of this work provide four major contributions to the field of ALL research:

1. Design and implementation of new methods to use absolute pressure sensor-based ALLs able to function under a broader spectrum of hydrodynamic conditions, including field measurements.
2. Development of a novel method for using high sensitivity air differential pressure sensors in artificial lateral lines.
3. Enabling real-time ALL velocity estimations (> 10 Hz) suitable for use in underwater robots in addition to improve several ALL functional characteristics, including sensitivity, reduction of atmospheric noise and power consumption (< 10 mW) as well as the overall payload size and mass.
4. Creation of a field-ready flow measurement tool capable of better hydraulic fish preference estimates ($R^2 = 0.817$) than a standard acoustic Doppler velocimeter ($R^2 = 0.585$). This may be explained by the distributed sensing capabilities and the higher sampling rate of the ALLs (25 Hz vs 200 Hz). However, further studies are necessary to confirm these results and establish direct relations.

Lühikokkuvõte

Veevoolu tajumine rõhusensoritel baseeruvate küljejooneanduritega: laborist välikatseteni

Looduslik vee liikumine varieerub globaalsetest temperatuuri- ning tuulemõjust põhjustatud hoovustest kuni väikeste jõevoolus kividelt eralduvate keeristeni. Vastavalt on ka vees elavatel liikidel looduslike veevooludega adapteerumiseks arenenud märkimisväärne amplituud erinevaid veevoolu tajumise tehnikaid. Üheks enim uuritud bioloogiliseks veevoolu tajuvaks organiks on kalade octavolaterais afferent system, nimetatakse tihti ka „küljejooneorganiks“ kuna paikneb piki kala külgi. Küljejooneorgani abil saavad kalad teostada erinevaid käitumismustreid nagu vastuvoolu ujumine, parves liikumine, röövloomade ning takistuse vältimine ning saakloomade tuvastamine. Selle meetodid efektiivsus ning kasu erineva keerukusega veevooludes on inspireerinud teadlasi arendama kunstlikku küljejooneandurit (KKA). KKA-i laialdasema rakendamine võimaldaks uudselt teostada naturaalsete veevoolude mõõtmisi ning klassifitseerimist, võimaldaks uurida veeliikide elukeskkondi ning parandada veealuste robotite tajumisvõimet. Paraku KKA rakendused piirnenud seni laborikatsetega.

Antud väitekirja eesmärgiks on vabastada KKA-d laboritingimustest, luues selleks keskkonnauuringute ning veealuse robotika tarvis välitingimustesse sobiva KKA. Andud väitekirja on seetõttu ka tugevalt interdistsiplinaarne, ühendades omavahel robotika, bioloogiast inspireeritud sensorika, ökoloogia ning hüdrodünaamika. Töö eesmärkideni jõuti kolme sammuga, järgides inkrementaalse arenduse põhimõtet.

Esimese sammuna (2. peatükk) uuriti absoluutrõhusensoritel baseeruvaid state-of-art KKA tööd. Esmase KKA evaluatsioonitöö välja kriitilised piirangud praktiliste rakenduste teostamiseks. Antud piirangute ületamiseks töötati välja uued algoritmid ning leiti katseliselt, pool-empiriiliselt seosed veevoolu suuruste (kiiruse ja turbulentsuse) hindamiseks. Antud uued meetodid, võrreldes olemasolevate KKA meetoditega, võimaldavad veevoolu täpselt määrata sõltumata kalibreerimisprotseduurist ning veevoolu suuna kõrvalekalletest. Pakutud uued algoritmid ning meetodid laiendavad KKA-te rakendusvaldkondi hüdrodünaamikas, kaasa arvatud katsetel välitingimustes. Esimese lähenduse suurimaks puuduseks oli andmete järeltöötluse vajadus, mis ei võimaldanud KKA-st lugemeid saada mõõtmiste tegemisel hetkel.

Reaalajas andmete saamine on oluline KKA veealuse robotika rakendustes, kus otsuseid tuleb vastu võtta vastavalt muutuvale keskkonnale. Seetõttu sai teiseks uurimissammuks antud töös (3. peatükk) tundlikel ning kiiretel õhudiferentsiaal-rõhusensoritel baseeruvate uude reaalaja KKA-te arendamine. Antud arendus eemaldas ka puudused ning piirangud, mis tulenesid esimeses lähenduses kasutatud absoluutrõhusensoritest. Diferentsiaal KKA omab automaatset kalibratsiooni, parendatud sügavusest ning välisrõhu muutusest sõltumatut tundlikust. Teise arendusetapi tulemusena valmis reaalajas toimiv diferentsiaal-KKA. Lisaks sellele, testimise ning valideerimise tulemusena saadi empiiriline mudel, mis annab täpseid hetkkiiruse lugemeid sõltumata voolusuunanurga kõrvalekalletest. Üheks suurimaks saavutuseks teises arendusfaasis võib pidada asjaolu, et õhudiferentsiaal-sensoritel baseeruva KKA-ga tõsteti tundlikkust 10000% võrreldes esimeses arendusetapis kasutatud absoluutrõhusensoritel baseeruva lahendusega.

Diferentsiaal-KKA-ga lahendati probleemid, mis ilmnesisid esimeses lähenduses kasutatud absoluutrõhuanduritega. Seega viimase sammuna (4. peatükis) antud töös

keskendutakse rakendustele koos kalibreerimise, testimise ning valideerimisega. Täpsemalt toodi välja kaks rakendusvaldkonda, (1) reaajas veealuste robotite kiiruse hindamine ning (2) kalade hüdrauiliste eelistuste iseloomustamine vertikaalsete piludega kalapääsudes. Mõlema valdkonna puhul võrreldi KKA sooritust etalonandmete vastu ning näidati pakutud lahenduse edasiarenduse ulatust võrreldes olemasolevate meetoditega.

Antud töö tulemused annavad neli suuremat panust KKA teadustöösse;

1. Absoluutrõhusensoritel baseeruvate KKA-te uudsete meetodikate arendus ning kasutuselevõtt laiendamaks nende rakendusvaldkondi hüdrodünaamikas ning välitingimustes.
2. Uudse kõrge tundlikkusega õhu-diferentsiaalrõhusensoritel baseeruva kunstliku kala-küljejooneanduri väljatöötamine.
3. KKA-ga reaajas veevoolu kiiruse mõõtmismetoodika teostus (>10 Hz), mis on rakendatav allveerobotikas. Lisaks mitme KKA funktsionaalse aspekti parendamine, sealhulgas tundlikkuse tõstmine, atmosfäärist tingitud müra ning energia tarbimise (< 10mW) vähendamine, seadme suuruse ning kaalu alandamine.
4. Välitingimustes sobiliku veevoolu mõõtmisvahendi loomine, mis võimaldab hinnata kalade hüdrauilisi eelistusi ($R^2 = 0.817$) paremini kui standardina kasutatav akustiline Doppleri kiirusemõõtja ($R^2 = 0.585$). Antud asjaolu on seletatav KKA hajutatud mõõtmismeetodi ning kõrgema diskreetimissagedusega (25 Hz vs 200 Hz). Antud väite kinnitamiseks ning otseste seoste loomiseks on siiski vaja läbi viia täiendavaid uuringuid.

Appendix 1

Publication I

Fuentes-Pérez, J. F., Tuhtan, J. A., Carbonell-Baeza, R., Musall, M., Toming, G., Muhammad, N., & Kruusmaa, M. (2015). *Current velocity estimation using a lateral line probe*. *Ecological Engineering*, 85, 296–300. DOI: 10.1016/j.ecoleng.2015.10.008.

Appendix 2

Publication II

Strokina, N., Kämäräinen, J. K., Tuhtan, J. A., Fuentes-Pérez, J. F., & Kruusmaa, M. (2016). *Joint estimation of bulk flow velocity and angle using a lateral line probe*. IEEE Transactions on Instrumentation and Measurement, 65(3), 601–613. DOI: 10.1109/TIM.2015.2499019.

Appendix 3

Publication III

Tuhtan, J. A., Fuentes-Pérez, J. F., Strokina, N., Toming, G., Musall, M., Noack, M., Kämäräinen, J. K., & Kruusmaa, M. (2016). *Design and application of a fish-shaped lateral line probe for flow measurement*. Review of Scientific Instrumentation. DOI: 10.1063/1.4946765.

Appendix 4

Publication IV

Tuhtan, J. A., Fuentes-Pérez, J. F., Toming, G. & Kruusmaa, M. (2017). *Flow velocity estimation using a fish-shaped lateral line probe with product-moment correlation features and a neural network*. Flow Measurement and Instrumentation, 54, 1–8. DOI: 10.1016/j.flowmeasinst.2016.10.017.

Appendix 5

Publication V

Fuentes-Pérez, J. F., Kalev, K., Tuhtan, J. A., & Kruusmaa, M. (2016). *Underwater vehicle speedometry using differential pressure sensors: Preliminary results*. IEEE OES Autonomous Underwater Vehicles. DOI: 10.1109/AUV.2016.7778664.

Appendix 6

Publication VI

Chen, K., Tuhtan, J. A., Fuentes-Pérez, J. F., Toming, G., Musall, M., Strokina, N., Kämäräinen, J. K., & Kruusmaa, M. (2017). *Estimation of flow turbulence metrics with a lateral line probe and regression*. IEEE Transactions on Instrumentation and Measurement, 66(4), 651–660. DOI: 10.1109/TIM.2017.2658278.

Appendix 7

Publication VII

Fuentes-Pérez, J. F., Muhammad, N., Tuhtan, J. A., Carbonell-Baeza, R., Musall, M., Toming, G., & Kruusmaa, M. (2017). *Map-based localization in structured underwater environment using simulated hydrodynamic maps*. IEEE ROBOTICS AND AUTOMATION 2017. DOI: 10.1109/ROBOT.2017.8324406.

Appendix 8

Publication VII

Fuentes-Pérez, J. F., Christian Meurer, Tuhtan, J. A., & Kruusmaa, M. (2018). *Differential pressure sensors for underwater speedometry in variable velocity and acceleration conditions*. IEEE OES Journal of Oceanic Engineering. DOI: 10.1109/JOE.2017.2767786.

Curriculum vitae

Personal data

Name: Juan Francisco Fuentes-Pérez
Date of birth: 18.12.1985
Place of birth: Gernika, Bizkaia
Citizenship: Spanish

Contact data

E-mail: jffuentesperez@gmail.com

Education

2014–2019 Tallinn University of Technology – PhD
2012–2013 University of Valladolid – MSC, Engineering for Agroforestry
Development
2009–2012 University of Valladolid – BSC, Forestry Engineer
2004–2009 University of Valladolid – BSC, Forestry Technical Engineer
2001–2003 Gernika BHI – High school

Language competence

English – Fluent
Spanish – Native
Basque – Native

Professional employment

2014–2019 Tallinn University of Technology - Junior Researcher
2010–2014 University of Valladolid, TU Hydraulic and Hydrology – Engineer

Elulookirjeldus

Isikuandmed

Nimi: Juan Francisco Fuentes-Pérez
Sünniaeg: 18.12.1985
Sünnikoht: Gernika, Bizkaia
Kodakondsus: Hispaania

Kontaktandmed

E-post: jffuentesperez@gmail.com

Hariduskäik

2014–2019 Tallinna Tehnikaülikool – PhD
2012–2013 Valladolid Ülikool – MSC, Engineering for Agroforestry Development
2009–2012 Valladolid Ülikool – BSC, Forestry Engineer
2004–2009 Valladolid Ülikool – BSC, Forestry Technical Engineer
2001–2003 Gernika BHI – High school

Keelteoskus

Inglise keel – Kõrgtase
Hispaania keel – Emakeel
Baski keel – Emakeel

Teenistuskäik

2014–2019 Tallinna Tehnikaülikool – Nooremteadur
2010–2014 Valladolid Ülikool, TU Hydraulic and Hydrology – Engineer